

# 1 Reply to Referees

## 1.1 Referee 1

We thank the referee for his/her useful comments. We have included the referee's comments (*italics*) and comments specific replies (AC) below. The corresponding changes made in the manuscript are written in blue below the ACs.

*This paper presents an inversion of CH<sub>4</sub> and CO<sub>2</sub> using GOSAT column retrievals and surface observations. The central theme of the paper is a comparison of flux inversions derived from an assimilation of the XCH<sub>4</sub>/XCO<sub>2</sub> ratio (also constrained by surface observations) to proxy or surface only retrievals. The paper is suitable for publication in ACP, provided that some of the comments below are addressed.*

### General Comments:

- *Use of bias correction. As the authors themselves note (P18, line 29), there appears to be a double counting of the surface observations in the satellite inversions, because a bias correction has been applied, based on previous satellite-only and surface-only inversions. In addition to this double-counting, I suggest that there are two problems with this approach:*

*a) any discrepancy between these two inversions is likely to be indicator of systematic model errors, which are likely to result in a relatively complex offset between two such inversions (indeed, this appears to be indicated in Figure 12). Therefore, the use of a linear correction would leave out some potentially important features un-accounted for;*

AC: Previous analyses have shown that systematic errors are likely caused by a combination of errors in the transport model and the GOSAT retrievals (Monteil et al., 2013). It is better to take them out to avoid that these errors impact the fluxes. We agree with the reviewer that our approach of using a linear bias correction may leave some important features unaccounted. At the same time, using a higher order bias correction can also remove some of the information content of the GOSAT measurements. Linear bias correction is not an unsuitable choice keeping in mind the trade-off.

*b) any uncertainty associated with this correction is not propagated through the inversion. Instead of imposing this correction as a hard constraint, why not include it in the inversions? Point a) above could also be addressed by disaggregating this potential error into more than two components (i.e. an intercept and a gradient).*

AC: Optimizing the corrections further in the inversion will lead to a compromise between fluxes and bias adjustments. We do not trust this component of the flux adjustment, as it might be different for the proxy and

ratio inversions that we want to compare. It would add further complexity to our analysis.

- *Uncertainty quantification.* Given the rather extensive discussion of potential biases and uncertainties associated with the retrievals and the model, the uncertainties derived in Figures 3, 4, 5 and 7 seem very optimistic to me. I think the paper would benefit from a much broader discussion about any limitations in the uncertainty quantification methods employed in this paper (preferably with reference to other methods that have been used in the literature). This should also include a discussion of the choices made about the a priori uncertainties. For example, it appears that a choice of 50% uncertainty for each grid cell for the CH<sub>4</sub> prior was used with a temporal correlation of 3 months and length scale of 500 km. Why were these figures chosen? What might be the influence on the inversion of choices of this nature? When aggregated together, it appears that this uncertainty leads to a prior uncertainty on continental scales of about 5-10% (Figure 3). Does this seem realistic? It seems small to me, especially since it is apparently inconsistent with the outcome of the inversion for several regions. There are several systematic factors that could also strongly influence the outcome of the inversion (e.g. convection, OH uncertainty), which should be discussed.

AC: It is hard to guess the true uncertainty of the prior fluxes. We take 50% as  $1\sigma$  in each grid. If the min/max values are at 95% confidence (i.e.  $2\sigma$ ), our fluxes range between 0 and twice the mean. The correlation lengths help to transfer the uncertainties to larger scales. Earlier studies like Fraser et al., (2013) have also used similar (5-10%) prior uncertainty on continental scales.

The balance between adjustments made to CH<sub>4</sub> and CO<sub>2</sub> fluxes in the RATIO inversion is also an important factor in our setup. With our present values, the Xratio measurements are twice sensitive to  $1\sigma$  changes in CH<sub>4</sub> than CO<sub>2</sub>. As the inversion adjusts the fluxes with respect to the square of modelobservation mismatches in the Bayesian framework, CH<sub>4</sub> fluxes are adjusted  $2^2 = 4$  times more than CO<sub>2</sub> fluxes (please see our reply to the 1st comment of 2nd reviewer). If we increase the CH<sub>4</sub> prior uncertainty, this number will become even higher making the CO<sub>2</sub> fluxes too restricted.

We have made the following update to our manuscript (Discussion Section) to address the optimistic estimates of posterior uncertainties:

It is noteworthy that the inversions are run assuming uncorrelated measurements and a perfect transport. Also, as we are not optimizing the atmospheric sink of CH<sub>4</sub>, all the information from its budget is used to constrain the surface fluxes. Hence, the estimates of posterior uncertainties tend to be optimistic in this study. The  $\chi^2$  statistic indicates whether the assumed measurement and prior errors are statistically consistent (Meirink et al., 2008). We find  $\chi^2/n_s = 0.93$  for RATIO, 0.96 for PR-CT, 0.93 for PR-LM and 1.14 for SURF in the CH<sub>4</sub> inversions ( $n_s$  is the number of observa-

tions assimilated in the inversion). This shows that we are not drastically underestimating the prior uncertainties in our CH<sub>4</sub> inversions.

**Minor Comment:**

- P2 L5: *still consistent results are obtained. Consistent with respect to what?*

still consistent results are obtained with respect to other CH<sub>4</sub> inversions.

- P2 L10: *original information? Im not sure what this means.*

Atmospheric measurements of GHGs can provide information about their atmospheric budget. Inverse modeling methods, also known as top-down approaches, have been developed to make use of this information to obtain improved estimates of surface fluxes

- P4, Section 2: *This could do with a brief overview of the chemical transport model setup (fluxes, OH fields, dynamics, etc).*

AC: we have added the following to our manuscript (in method section):

We use the TM5-4DVAR inversion modeling system. It is comprised of the Tracer Transport Model version 5 (TM5, Krol et al., 2005) coupled to a variational data assimilation system (4DVAR, Meirink et al., 2008). TM5 simulates the spatiotemporal distribution of a tracer in the atmosphere for a given set of fluxes. In this study, TM5 is run at a 64 degree horizontal resolution and 25 vertical hybrid sigma pressure levels from the surface to the top of the atmosphere. The meteorological fields for this offline model are taken from the European Centre for Medium-Range Weather Forecasts (ECMWF) ERA-interim reanalysis [Dee et al., 2011].

- P5 L4:7. *Are these choices largely subjective? Reasons should be given, and a discussion of the implications. See general comment above.*

AC: Please refer to our reply to the general comment above.

- P5 L14: *Missing full stop before The RemoTeC*

- P5 L18: *referred to as*

- P5 L25: *Use of additional here. . . additional to what (I presume it means in addition to the TCCON bias correction, which is described in the section below).*

- P8 L1: *Use of uncorrelated observation/model errors. Is it realistic to assume that the observation and model representation errors are uncorrelated in space and time? What might be the implications of this choice?*

AC: A Bayesian inverse model should in principle address the correlation of observations and weight them properly. The observations are assimilated in the inversion by comparing them with model-simulated mixing ratios. Therefore, errors in the model can also create a correlation. In practice, correlations are often ignored, both because they are difficult to quantify, and properly taking them into account slows down the inversion systems by a large extent. A prominent illustration of this is given by the numerical weather prediction systems since most of them assume uncorrelated

observation errors (but correlated prior errors). Inverse modeling studies of CH<sub>4</sub> don't take them into account directly (for example, Alexe et al., 2014, Houweling et al., 2014, Monteil et al., 2013). Studies assimilating SCIAMACHY measurements implemented the binning method to reduce the impact of clustered measurements of SCIAMACHY (Houweling et al., 2014, Monteil et al., 2013). However, this is not so critical for GOSAT, as the number of soundings is lesser in amount. Also, the main goal of this study is to compare the results of different inversion methods in a consistent setup. All the inversions are done assuming uncorrelated observation/model errors, so this should not affect our results drastically.

- P8 L18: *Re-word relatively less errors is not grammatically correct.*
- P11 L9: *do not show an important seasonal dependence. This needs re-wording. I don't understand what an important seasonal dependence means.*
- P11 L18: *information that is used (remove comma).*
- P17 L18: *poorer rather than lesser*
- P21 L4: *Isn't it fairer to say that they largely cancel out? The cancellation is not 100%.*
- P23 L8: *Isn't 5x5 degrees quite a large area? Can this analysis be carried out over smaller scales?*

AC: 5x5 degrees area provides us with a sufficient number of GOSAT retrieval around the TCCON sites.

AC: All other minor comments are addressed in the revised manuscript.

## References:

- Alexe, M., Bergamaschi, P., Segers, A., Detmers, R., Butz, A., Hasekamp, O., Guerlet, S., Parker, R., Boesch, H., Frankenberg, C., Scheepmaker, R. A., Dlugokencky, E., Sweeney, C., Wofsy, S. C., and Kort, E. A.: Inverse modeling of CH<sub>4</sub> emissions for 2010/2011 using different satellite retrieval products from GOSAT and SCIAMACHY, *Atmospheric Chemistry and Physics Discussions*, 14, 11 49311–539, doi:10.5194/acpd-14-11493-2014.
- Dee, D. P., Uppala, S. M., Simmons, A. J., Berrisford, P., Poli, P., Kobayashi, S., Andrae, U., Balmaseda, M. A., Balsamo, G., Bauer, P., Bechtold, P., Beljaars, A. C. M., van de Berg, L., Bidlot, J., Bormann, N., Delsol, C., Dragani, R., Fuentes, M., Geer, A. J., Haimberger, L., Healy, S. B., Hersbach, H., Holm, E. V., Isaksen, I., Kllberg, P., Kllner, M., Matricardi, M., McNally, A. P., Monge-Sanz, B. M., Morcrette, J.-J., Park, B.-K., Peubey, C., de Rosnay, P., Tavolato, C., Thpaut, J.-N., and Vitart, F.: The ERA-Interim reanalysis: configuration and performance of the data assimilation system, *Q. J. Roy. Meteor. Soc.*, 137, 553597, doi:10.1002/qj.828, 2011.
- Fraser, A., Palmer, P. I., Feng, L., Boesch, H., Cogan, A., Parker, R., Dlugokencky, E. J., Fraser, P. J., Krummel, P. B., Langenfelds, R. L.,

ODoherty, S., Prinn, R. G., Steele, L. P., van der Schoot, M., and Weiss, R. F.: Estimating regional methane surface fluxes: the relative importance of surface and GOSAT mole fraction measurements, *Atmos. Chem. Phys.*, 13, 56975713, doi:10.5194/acp-13-5697-2013, 2013.

Houweling, S., Krol, M., Bergamaschi, P., Frankenberg, C., Dlugokencky, E. J., Morino, I., Notholt, J., Sherlock, V., Wunch, D., Beck, V., Gerbig, C., Chen, H., Kort, E. a., Rckmann, T., and Aben, I.: A multi-year methane inversion using SCIAMACHY, accounting for systematic errors using TC-CON measurements, *Atmospheric Chemistry and Physics*, 14, 39914012, doi:10.5194/acp-14-3991-2014.

Krol, M., Houweling, S., Bregman, B., van den Broek, M., Segers, A., van Velthoven, P., Peters, W., Dentener, F., and Bergamaschi, P.: The two-way nested global chemistry-transport zoom model TM5: algorithm and applications, *Atmos. Chem. Phys.*, 5, 417 432, doi:10.5194/acp-5-417-2005, 2005.

Meirink, J. F., Bergamaschi, P., and Krol, M. C.: Technical Note: Four-dimensional variational data assimilation for inverse modelling of atmospheric methane emissions: method and comparison with synthesis inversion, doi:10.5194/acpd-8-12023-2008, 2008.

Monteil, G., Houweling, S., Butz, A., Guerlet, S., Schepers, D., Hasekamp, O., Frankenberg, C., Scheepmaker, R., Aben, I., and Rckmann, T.: Comparison of CH<sub>4</sub> inversions based on 15 months of GOSAT and SCIAMACHY observations, *Journal of Geophysical Research: Atmospheres*, 118, 11,80711,823, doi:10.1002/2013JD019760.

## 1.2 Referee 2

We thank the referee for his/her useful comments. We have included the referee's comments (*italics*) and comments specific replies (AC) below. The corresponding changes made in the manuscript are written in [blue](#) below the ACs.

*The study by S. Pandey and coauthors reports inverse modeling experiments testing use of the GOSAT-retrieved ratio of methane and carbon dioxide column average concentrations for inverse modeling of both CO<sub>2</sub> and CH<sub>4</sub> surface fluxes. The manuscript does present new results of considerable interest, and can be accepted with a minor revision. Technical correction and proofreading is needed as there are many mistypes.*

### Detailed Comments:

*The ratio in hand is composed of 2 variables that vary very little around mean values. Linear expansion around mean state will transform the difference to a linear combination of XCO<sub>2</sub> and XCH<sub>4</sub>, that is  $d(XCH_4/XCO_2) = (dXCH_4 - dXCO_2 * XCH_4/XCO_2)/XCO_2$ . Given the ratio of column mean concentration around 400/1.7 ppm/ppm, XCH<sub>4</sub> gets about 200 times higher weight in the linear combination of the two. Mysteiously, the ratio of the XCO<sub>2</sub> and XCH<sub>4</sub> errors is about same order (2/0.012 ppm/ppm), so the correlated parts of the errors are largely cancelled in ratio. On the other hand, ratio of surface fluxes is in order of 10/0.3=30 for anthropogenic (according to EDGAR data), and 9/0.2=18 GtC/GtC for natural fluxes (growing season net flux by Randerson et al. 1996; wetlands in Melton et al. 2013). Thus, we have ample imbalance of 6-10 times in favor of methane in terms of signal to noise ratio for sensitivity of XCH<sub>4</sub> to XCO<sub>2</sub> ratio to surface fluxes. Accordingly, use of a retrieved ratio for CH<sub>4</sub> flux inversion is better justified than application for CO<sub>2</sub> flux inversion. That makes results of this study interesting to look in. In particular, latitude dependent XCH<sub>4</sub> bias contributed by combination of model (stratosphere) and retrieval biases comes in place of reduced aerosol and cloud effects. It would be useful to add discussion on the contribution of the methane XCH<sub>4</sub> biases to CO<sub>2</sub> inversion constrained by XCH<sub>4</sub>/XCO<sub>2</sub> ratio.*

AC: We agree with the reviewer, however, there are some limitations to the calculation done above. In our inversions, we do not optimize anthropogenic CO<sub>2</sub> fluxes. Also, the fluxes are weighted with their respective error in the cost function. We calculate the same number by adding a  $1\sigma$  perturbation of global CH<sub>4</sub> ( $\approx 15$  Tg/yr) and CO<sub>2</sub> (1.2 GtC/yr) fluxes in the atmosphere. This will have the corresponding change in the mixing ratio of the tracers in the atmosphere. The change in CH<sub>4</sub> mixing ratio will be  $(1800 \text{ ppb} \times (15 \text{ Tg.yr}^{-1}/5000 \text{ Tg})) = 5.4 \text{ ppb.yr}^{-1} = 0.3\%.\text{yr}^{-1}$ . For CO<sub>2</sub>, it will be  $(400 \text{ ppm} \times 1.30 \text{ PgC.yr}^{-1}/860 \text{ PgC}) = 0.6 \text{ ppm.yr}^{-1} = 0.15 \text{ \%}.\text{yr}^{-1}$ . So the Xratio will be impacted 0.3/0.15 = 2 times more due to CH<sub>4</sub> than CO<sub>2</sub>.

As the inversion is adjusted with the square of the observations, CH<sub>4</sub> fluxes will be adjusted  $2^2 = 4$  times more than CO<sub>2</sub> fluxes. However, this number can be different on regional scales. As CO<sub>2</sub> and CH<sub>4</sub> surface data are assimilated also and both of them receive approximately equal weight in the inversion, the ratio may be lower. We have added the following to the revised manuscript:

The signal from Xratio can be up to  $\approx 4$  times more sensitive to adjustment of CH<sub>4</sub> fluxes than CO<sub>2</sub> fluxes in our inversion setup. In such case, the surface observations of CO<sub>2</sub> become the primary constraint on the CO<sub>2</sub> fluxes. This can be further verified by looking at Supplementary figure 2, in which the RATIO and SURF inversion show very good agreement. It should be also noted that latitude dependent XCH<sub>4</sub> bias contributed by the combination of transport model and retrieval biases become more important in a Xratio inversion while errors reduce due to aerosol and cloud scattering.

#### Technical corrections:

*Page 01- Line 03 Putting here "biased" instead of "heavily biased" would suffice, referring to current state of retrievals.*

*02-17 and 02-25 Lists of papers are similar, likely to present same information twice, better to put some distinction. Adding Deng et al ACP 2014 and Maksyutov et al ACP 2013 may be useful for completeness.*

*02-31 two types of retrieval methods can be used in place of two retrieval methods*

*03-21 (Fraser et al., 2014) -> Fraser et al., (2014)*

*04-27 As- sessment -> Assessment*

*04-26 right spell should be v.4.2 FT2010*

*05-01 onJacobson -> on Jacobson*

*05-12 adding reference to Remotec (Butz?) would help here.*

*08-04 GOSAST -> GOSAT.*

*08-20 Should ppm/ppm be used in place of ppb/ppm?*

*09-01 Units of table 1 need more explanation. Text says it is percentage difference weighted with GOSAT+TCCON error, the value doesnt look like percentage.*

*25-01 inChevallier -> in Chevallier*

*28-31 In the reference list initials like A. are appearing as a. in multiple locations. AC: All technical corrections are addressed in the revised manuscript.*

#### 1.2.1 References

Randerson, J. T. and coauthors, Substrate limitations for heterotrophs: Implications for models that estimate the seasonal cycle of atmospheric CO<sub>2</sub>, Global Biogeochem. Cycles, 10(4), 585602, doi:10.1029/96GB01981, 1996.

Melton, J. R., and coauthors, Present state of global wetland extent and wetland methane modelling: conclusions from a model inter-comparison project (WETCHIMP), *Biogeosciences*, 10, 753-788, doi:10.5194/bg-10-753-2013, 2013.



# Inverse modeling of GOSAT-retrieved ratios of total column CH<sub>4</sub> and CO<sub>2</sub> for 2009 and 2010.

S. Pandey<sup>1,2</sup>, S. Houweling<sup>1,2</sup>, M. Krol<sup>1,2,3</sup>, I. Aben<sup>2</sup>, F. Chevallier<sup>4</sup>, E. J. Dlugokencky<sup>5</sup>, L. V. Gatti<sup>6</sup>, M. Gloor<sup>7</sup>, J. B. Miller<sup>5,8</sup>, R. Detmers<sup>2</sup>, T. Machida<sup>9</sup>, and T. Röckmann<sup>1</sup>

<sup>1</sup>Institute for Marine and Atmospheric Research Utrecht, Utrecht University, Utrecht, the Netherlands

<sup>2</sup>SRON Netherlands Institute for Space Research, Utrecht, the Netherlands

<sup>3</sup>Wageningen University, Wageningen, the Netherlands

<sup>4</sup>Laboratoire des Sciences du Climat et de l'Environnement (LSCE), CEA CNRS UVSQ, IPSL, Gif-sur-Yvette, France

<sup>5</sup>NOAA Earth System Research Laboratory, Boulder, Colorado, USA

<sup>6</sup>Instituto de Pesquisas Energéticas e Nucleares (IPEN), Centro de Química Ambiental, São Paulo, Brazil

<sup>7</sup>School of Geography, University of Leeds, Leeds, UK

<sup>8</sup>Cooperative Institute for Research in Environmental Sciences (CIRES), University of Colorado, Boulder, Colorado, USA.

<sup>9</sup>National Institute for Environmental Studies, Tsukuba, Japan

*Correspondence to:* S. Pandey (s.pandey@uu.nl)

## Abstract.

This study investigates the constraint provided by greenhouse gas measurements from space on surface fluxes. Imperfect knowledge of the light path through the atmosphere, arising from scattering by clouds and aerosols, can ~~heavily bias~~ create biases in column measurements retrieved from space. To minimize the impact of such biases, ratios of total column retrieved CH<sub>4</sub> and CO<sub>2</sub> ( $X_{\text{ratio}}$ ) have been used. We apply the ratio inversion method described in Pandey et al. (2015) to retrievals from the Greenhouse Gas Observing SATellite (GOSAT). The ratio inversion method uses the measured  $X_{\text{ratio}}$  as a weak constraint on CO<sub>2</sub> fluxes. In contrast, the more common approach of inverting proxy CH<sub>4</sub> retrievals (Frankenberg et al., 2005) prescribes atmospheric CO<sub>2</sub> fields and optimizes only CH<sub>4</sub> fluxes.

The TM5-4DVAR inverse modeling system is used to simultaneously optimize the fluxes of CH<sub>4</sub> and CO<sub>2</sub> for 2009 and 2010. The results are compared to proxy inversions using model-derived-XCO<sub>2</sub> mixing ratios ( $XCO_2^{\text{model}}$ ) from CarbonTracker and MACC. The performance of the inverse models is evaluated using aircraft measurements from the HIPPO, CONTRAIL and AMAZONICA projects.

$X_{\text{ratio}}$  and  $XCO_2^{\text{model}}$  are compared with TCCON retrievals to quantify the relative importance of errors in these components of the proxy  $XCH_4$  retrieval ( $XCH_4^{\text{proxy}}$ ). We find that the retrieval errors in  $X_{\text{ratio}}$  (mean = 0.61 %) are generally larger than the errors in  $XCO_2^{\text{model}}$  (mean = 0.24 % and 0.01% for CarbonTracker and MACC, respectively). On the annual time scale, the CH<sub>4</sub> fluxes from the different satellite inversions are generally in agreement with each other, suggesting that errors in  $XCO_2^{\text{model}}$  do not limit the overall accuracy of the CH<sub>4</sub> flux estimates. On the seasonal time scale, however, larger differences are found due to uncertainties in  $XCO_2^{\text{model}}$ , particularly over Australia and in the tropics. The ratio method stays closer to the *a priori* CH<sub>4</sub> flux in these regions, because it is capable of simultaneously adjusting the CO<sub>2</sub> fluxes. Over Tropical South America, comparison to independent measurements shows that CO<sub>2</sub> fields derived from the ratio method are less realistic than

those used in the proxy method. However, the  $\text{CH}_4$  fluxes are more realistic, because the impact of unaccounted systematic uncertainties is more evenly distributed between  $\text{CO}_2$  and  $\text{CH}_4$ . The ratio inversion estimates an enhanced  $\text{CO}_2$  release from Tropical South America during the dry season of 2010, which is in accordance with the findings of Gatti et al. (2014) and Vanderlaan et al. (2015).

5 The performance of the ratio method is encouraging, because despite the added non-linearity due to the assimilation of  $X_{\text{ratio}}$  and the significant increase in the degree of freedom by optimizing  $\text{CO}_2$  fluxes, still consistent results are obtained with respect to other  $\text{CH}_4$  inversions.

## 1 Introduction

Detailed knowledge of the global distribution of surface fluxes of potent greenhouse gases (GHGs) such as  $\text{CH}_4$  and  $\text{CO}_2$  is needed to investigate the uncertain feedback of the global carbon cycle to human disturbances. Atmospheric measurements of these GHGs ~~provide original information about surface fluxes~~ can provide information about the atmospheric budget. Inverse modeling methods, also known as top-down approaches, have been developed to make use of that information to obtain improved estimates of surface fluxes. Bottom-up estimates of those fluxes are used as prior values in the top-down method, and are further improved using atmospheric measurements. Inversions assimilating flask and/or *in-situ* measurements from surface networks have significantly improved our knowledge of the sources and sinks of GHGs (Bousquet et al., 2006; Bergamaschi et al., 2010; Hein et al., 1997; Houweling et al., 1999; Peters et al., 2007; Chevallier et al., 2010; Gurney et al., 2008). However, many regions with a key role in the global annual budgets of  $\text{CO}_2$  and  $\text{CH}_4$  are not adequately covered by the surface measurement network. This is especially true for tropical regions and the Southern Hemisphere. ~~Total column measurements of  $\text{CH}_4$  and  $\text{CO}_2$  ( $\text{XCH}_4$  and  $\text{XCO}_2$ ) by sensors onboard satellites, with near global coverage, have been used in some recent studies (Basu et al., 2013; Fraser et al., 2013; Houweling et al., 2014; Detmers et al., 2015; Basu et al., 2014).~~

The Greenhouse Gas Observing Satellite (GOSAT), launched in January 2009 by the Japanese Space Agency (JAXA), is the first satellite dedicated to monitoring GHGs from space (Kuze et al., 2009; Yokota et al., 2009; Yoshida et al., 2011). Onboard are the Thermal And Near Infrared Sensor for carbon Observations-Fourier Transform Spectrometer (TANSO-FTS) and a dedicated Cloud and Aerosol Imager (TANSO-CAI). TANSO-FTS measures the absorption spectra of Earth reflected sunlight in the shortwave-infrared (SWIR) spectral range, from which  $\text{XCO}_2$  and  $\text{XCH}_4$  are retrieved with global coverage. Several inverse modeling studies have applied these measurements to derive constraints on the surface fluxes of  $\text{CH}_4$  and  $\text{CO}_2$  (Alexe et al., 2014; Basu et al., 2013; Bergamaschi et al., 2013; Fraser et al., 2013; Houweling et al., 2015; Monteil et al., 2013; Turner et al., 2014; (Alexe et al., 2014; Basu et al., 2013; Deng et al., 2014; Maksyutov et al., 2012; Bergamaschi et al., 2013; Fraser et al., 2013; Houweling et al., 2015; Monteil et al., 2013; Turner et al., 2014; Yokota et al., 2009; Yoshida et al., 2011).

Systematic errors in satellite retrievals are an important factor limiting the scientific interpretation of the data, and various methods have been proposed to mitigate their impact on the inferred surface fluxes (Bergamaschi et al., 2007; Frankenberg et al., 2005; Butz et al., 2010; Parker et al., 2015). An important source of systematic error is scattering of light by aerosols and thin cirrus clouds along the measured light path. Two types of retrieval methods have been developed in the past to account for atmospheric scattering, referred to as the “full-physics” and “proxy” approach. The full-physics approach tries to account

for scattering-induced errors by explicitly modeling the scattering process, and retrieving scattering properties from the data (Butz et al., 2010). The proxy method, first introduced by (Frankenberg et al., 2005), takes the ratio of  $XCH_4$  and  $XCO_2$  retrieved at nearby wavelengths (1562 to 1585 nm for  $XCO_2$  and 1630 to 1670 nm for  $XCH_4$ ) so that path length perturbations due to atmospheric scattering largely cancel out in the ratio (see equation 1).  $X_{ratio}$  is multiplied with model-derived- $XCO_2$  ( $XCO_2^{model}$ ) to derive  $XCH_4$  ( $XCH_4^{proxy}$ ) (see equation 2).

$$X_{ratio} = \frac{XCH_4^{ns}}{XCO_2^{ns}} \quad (1)$$

$$XCH_4^{proxy} = X_{ratio} \times XCO_2^{model} \quad (2)$$

Here,  $XCH_4^{ns}$  and  $XCO_2^{ns}$  are retrieved assuming a non-scattering atmosphere.  $XCO_2^{model}$  is calculated using a transport model, normally employing  $CO_2$  surface fluxes that have been optimized using surface measurements. The atmospheric  $CO_2$  fields are sampled at the coordinates of the satellite measurements and converted to corresponding total columns using the retrieval-derived averaging kernels (Schepers et al., 2012).

Proxy  $XCH_4$  retrievals from GOSAT have been used in many inverse modeling studies to investigate the global surface fluxes of  $CH_4$  (Alexe et al., 2014; Monteil et al., 2013; Fraser et al., 2013; Bergamaschi et al., 2013). These studies rely on the assumption that the uncertainties and biases in  $XCO_2^{model}$  are relatively unimportant. Some recent studies have investigated this assumption in further detail. Schepers et al. (2012) suggested that the errors in  $XCH_4^{proxy}$  are mostly dominated by the errors in  $XCO_2^{model}$ . Pandey et al. (2015) did a series of Observing System Simulation Experiments (OSSEs) to quantify the impact of errors in  $XCO_2^{model}$  on inversion-derived  $CH_4$  fluxes. It was concluded that the error becomes significant when  $CO_2$  fluxes are poorly constrained by the surface measurements. Parker et al. (2015) have estimated the uncertainty in  $XCO_2^{model}$  by comparing values from different models. They found that the uncertainty in  $XCO_2^{model}$  becomes the most important term in the error budget of  $XCH_4^{proxy}$  retrieval during summer months, when the satellite instrument operates under favorable illumination conditions allowing accurate determination of  $X_{ratio}$ .

In an attempt to avoid the biases introduced by errors in  $XCO_2^{model}$ , (~~Fraser et al., 2014~~) [Fraser et al. \(2014\)](#) developed the ‘ratio’ method, which simultaneously constrains  $CO_2$  and  $CH_4$  fluxes by assimilating  $X_{ratio}$  on the sub continental scale using the ensemble Kalman filter. Pandey et al. (2015) also developed a similar ratio inversion method for jointly optimizing the surface fluxes of  $CH_4$  and  $CO_2$  on the model grid scale using a variational optimization method. Fraser et al. (2014) compared posterior  $CH_4$  and  $CO_2$  flux uncertainties derived from a ratio inversion with traditional  $CH_4$  proxy and  $CO_2$  full-physics inversions and reported a larger reduction in uncertainty than the two in the tropics for the fluxes of both tracers.

This study extends the work of Pandey et al. (2015), by separately inverting real GOSAT measurements of  $X_{ratio}$  and  $XCH_4^{proxy}$  in a consistent and comparable framework to investigate the following questions: 1) How do errors in  $XCO_2^{model}$  influence the results of a  $XCH_4^{proxy}$  inversion? 2) How does the  $X_{ratio}$  inversion system developed by Pandey et al. (2015) perform using real data? The performance of the inversions is evaluated using independent aircraft measurements. We provide an

estimate of the posterior uncertainties of the  $X_{\text{ratio}}$  inverted fluxes using the Monte-Carlo method described by Chevallier et al. (2007).

This paper is organized as follows. The following section explains the methods used in this study. Subsection 2.1 describes the inverse model and the *a priori* flux assumptions. Subsection 2.2 lists the measurements that are assimilated in the inversions and used for validation. Subsection 2.3 provides an overview of the inversions performed in the study. Section 3 presents the inversion results and Section 4 discusses their implications for the use of satellite retrievals in inversion studies. Finally, we give the overall conclusions of this work.

## 2 Method

We invert GOSAT-retrievals of  $X_{\text{ratio}}$ , and  $X\text{CH}_4^{\text{proxy}}$ , each together with flask-air  $\text{CH}_4$  and  $\text{CO}_2$  measurements from the NOAA Global Greenhouse Gas Reference Network (GGGRN) to provide monthly surface fluxes of  $\text{CO}_2$  and  $\text{CH}_4$  using the TM5-4DVAR inversion system (Meirink et al., 2008). This is done as follows:

1. GOSAT-retrieved total column measurements of  $X_{\text{ratio}}$  are compared to measured ratios of  $X\text{CH}_4:\text{XCO}_2$  from the Total Carbon Column Observing Network (TCCON) of ground based sun-tracking Fourier Transform Spectrometers (FTSs) (Wunch et al., 2011).
2. GOSAT  $X_{\text{ratio}}$  measurements are bias corrected by fitting a linear function of surface albedo to the residual differences between GOSAT and TCCON. This done in  $X_{\text{ratio}}$  space.
3. GOSAT  $X_{\text{ratio}}$  measurements are multiplied by  $\text{XCO}_2^{\text{model}}$  to generate  $X\text{CH}_4^{\text{proxy}}$  measurements. Two different versions of  $\text{XCO}_2^{\text{model}}$  are used [see Section 2.2] to investigate the sensitivity to model errors.
4. The  $X\text{CH}_4^{\text{proxy}}$  and  $X_{\text{ratio}}$  measurements are inverted along with surface observations and the resulting posterior surface fluxes are integrated over the TRANSCOM regions (see supplementary Figure 4).
5. The posterior flux uncertainty for all inversions is quantified using a Monte-Carlo approach (see Appendix B) for consistent comparison.
6. The performance of the inversions is evaluated and compared using independent aircraft measurements.

The remainder of this section explains these steps in further detail.

### 2.1 Inversion setup

We use the TM5-4DVAR inversion modeling system. It is comprised of the Tracer Transport Model version 5 (TM5, Krol et al. (2005)) coupled to a variational data assimilation system (4DVAR, Meirink et al. (2008)). TM5 simulates the spatiotemporal distribution of a tracer in the atmosphere for a given set of fluxes. In this study, TM5 is run at a  $6^\circ \times 4^\circ$  degree horizontal resolution and 25 vertical hybrid sigma pressure levels from the surface to the top of the atmosphere. The meteorological fields for this

offline model are taken from the European Centre for Medium-Range Weather Forecasts (ECMWF) ERA-interim reanalysis Dee et al. (2011) .

CH<sub>4</sub> fluxes are optimized as a single flux category, representing the sum of all processes. For CO<sub>2</sub>, biospheric and oceanic fluxes are optimized separately. The *a priori* CH<sub>4</sub> fluxes used in the study are the same as used in Houweling et al. (2014), except for the Anthropogenic emissions. We use the ~~4.2v.4.2~~FT2010 versions-version of EDGAR (European Commission, Joint Research Centre (JRC)/Netherlands Environmental ~~As-sessment~~Assessment Agency), whereas Houweling et al. (2014) uses 4.1 version (<http://edgar.jrc.ec.europa.eu>). The *a priori* CO<sub>2</sub> fluxes come from CarbonTracker, CT2013B Peters et al. (2007), in which biosphere fluxes are based on the Carnegie-Ames-Stanford Approach (CASA) biogeochemical model (CASA), fire fluxes are based on Global Fire Emissions Database v3.1 (GFED) and ocean fluxes are based on Jacobson et al. (2007). Fossil fuel emissions in CarbonTracker are based on the Miller module ([http://www.esrl.noaa.gov/gmd/ccgg/carbontracker/CT2013B\\_doc.php#tth\\_sEc5](http://www.esrl.noaa.gov/gmd/ccgg/carbontracker/CT2013B_doc.php#tth_sEc5)) The *a priori* flux covariance matrix is constructed assuming relative flux uncertainties of 50%, 84% and 60% per grid box and month for the total CH<sub>4</sub>, biospheric CO<sub>2</sub>, and oceanic CO<sub>2</sub> categories, respectively. The fluxes are assumed to be correlated temporally using an exponential correlation function with temporal scales of 3, 3, and 6 months, respectively, and spatially with Gaussian functions using corresponding length scales of 500, 500 and 3000 km for total CH<sub>4</sub>, biospheric CO<sub>2</sub>, and oceanic CO<sub>2</sub>, respectively.

## 15 2.2 Measurements

Here we give a brief account of the measurements that were assimilated (GOSAT and NOAA) or used for validation (TCCON and aircraft-measurements).

### 2.2.1 GOSAT

The XCH<sub>4</sub><sup>ns</sup> and XCO<sub>2</sub><sup>ns</sup> terms in equation 1 were taken from the RemoTec XCH<sub>4</sub> Proxy retrieval v2.3.5 ([Butz et al., 2011](#)). More information about the dataset can be found in Product User Guide on the ESA GHG CCI website ([www.esa-ghg-cci.org/?q=webfm\\_send/180](http://www.esa-ghg-cci.org/?q=webfm_send/180)). The RemoTec algorithm uses GOSAT TANSO-FTS NIR and SWIR spectra to retrieve simultaneously XCH<sub>4</sub><sup>ns</sup> and XCO<sub>2</sub><sup>ns</sup> assuming a non-scattering atmosphere (Schepers et al., 2012). X<sub>ratio</sub> values were translated into XCH<sub>4</sub><sup>proxy</sup> using XCO<sub>2</sub><sup>model</sup> derived from the following: 1. Monitoring Atmospheric Composition and Climate (MACC) Re-analysis CO<sub>2</sub> product ([www.copernicus-atmosphere.eu](http://www.copernicus-atmosphere.eu)). It uses Laboratoire de Météorologie Dynamique transport model (LMDZ) (Chevallier, 2013). The corresponding XCH<sub>4</sub><sup>proxy</sup> product will be referred to as XCH<sub>4</sub><sup>ma</sup>. 2. CarbonTracker-2013B (<http://www.esrl.noaa.gov/gmd/ccgg/carbontracker/>). These CO<sub>2</sub> fields are calculated using the TM5 model as used in this study. The corresponding XCH<sub>4</sub><sup>proxy</sup> product will be referred to as XCH<sub>4</sub><sup>ct</sup>.

Both data assimilation systems optimized the CO<sub>2</sub> fluxes using surface measurements of CO<sub>2</sub>. For GOSAT measurements, we only used the high-gain soundings from GOSAT under cloud free conditions from nadir mode. This was done to avoid any systematic inconsistency among the operation modes of TANSO. Figure 1 shows the spatial coverage of the GOSAT dataset used in our inversions. Systematic mismatches between NOAA-optimized and GOSAT-optimized TM5 CH<sub>4</sub> fields were observed by Monteil et al. (2013). We apply ~~an additional bias correction to~~ another bias correction (in addition to

TCCON-based bias correction applied to  $X_{\text{ratio}}$  to  $X_{\text{ratio}}$  and  $X\text{CH}_4^{\text{proxy}}$  by comparing them to total column  $\text{CH}_4$  and  $\text{CO}_2$  optimized via an inversion using TM5-4DVAR and NOAA flask-air data (see Appendix A).

### 2.2.2 TCCON

TCCON is a global network of ground-based FTS instruments, for measuring the total column abundance of several gases, including  $X\text{CO}_2$  and  $X\text{CH}_4$ , in the near infrared region of the electromagnetic spectrum (Wunch et al., 2011). These measurements are the standard for validating total column retrievals from greenhouse gas observing satellites such as GOSAT. We validate  $X\text{CH}_4^{\text{ns}}$ ,  $X\text{CO}_2^{\text{ns}}$ ,  $X_{\text{ratio}}$ ,  $X\text{CO}_2^{\text{ma}}$ ,  $X\text{CO}_2^{\text{ct}}$  with corresponding values of  $X\text{CH}_4$ ,  $X\text{CO}_2$  and  $X\text{CH}_4:X\text{CO}_2$  measured by TCCON at 12 sites using the GGG2014 release of TCCON dataset (see Figure 1 and section 3.1). An albedo-based bias correction was applied to GOSAT-retrieved  $X_{\text{ratio}}$  to account for mismatch with TCCON  $X_{\text{ratio}}$  (see Appendix A).

### 2.2.3 NOAA

- High accuracy surface measurements of  $\text{CH}_4$  and  $\text{CO}_2$  were used from NOAA's GGGRN (<http://www.esrl.noaa.gov/gmd/ccgg/index.html>). The standard scales used for  $\text{CO}_2$  is the WMO X2007 scale and for  $\text{CH}_4$  is WMO X2004 scale. Only the sites with continuous data coverage (on a roughly weekly basis) without gaps in the time period of 1 June 2009 to 31 Dec 2010 were included. A total of 8552  $\text{CH}_4$  observations and 7843  $\text{CO}_2$  observations were used from the same 51 sites. Figure 1 shows the location of the observation sites.  $1\sigma$  uncertainties of 0.25 ppm and 1.4 ppb were assigned to  $\text{CO}_2$  and  $\text{CH}_4$  measurements, respectively (Basu et al., 2013; Houweling et al., 2014). Note that our system also assigns modeling errors to each observation, depending on simulated local gradients in mixing ratio (Basu et al., 2013). Modeling error values have a mean of 27.5 ppb, 2.72 ppm ( and  $1\sigma$  of 25.5 ppb, 4 ppm) for  $\text{CH}_4$  and  $\text{CO}_2$ , respectively.

### 2.2.4 Aircraft Measurements

- Airborne measurements from various aircraft measurement projects were used to test the inversion optimized model (see section 3.2.5). The following projects have been used:

1. HIAPER Pole-to-Pole Observations (HIPPO) from Wofsy et al. (2012a).
2. Comprehensive Observation Network for TRace gases by AIrLiner (CONTRAIL) from Machida et al. (2008).
3. IPEN aircraft measurements over Brazil (referred as AMAZONICA) from Gatti et al. (2014).

- HIPPO provides *in-situ* measurements covering the vertical profiles of  $\text{CO}_2$  and  $\text{CH}_4$  over the Pacific spanning a wide range in latitude (approximately pole-to-pole), from the surface up to the tropopause. We used data from the HIPPO 2 (October 26, 2009 to December 19, 2009) and HIPPO 3 (March 20, 2010 to April 20, 2010) campaigns. The continuous *in-situ* measurements of  $\text{CH}_4$  and  $\text{CO}_2$  that were used have been bias corrected with flask air samples that were collected during each flight and analyzed at NOAA (Wofsy et al., 2012b). This allows us to make consistent comparison with our inversions models, as all of them assimilate NOAA flask measurements. CONTRAIL makes use of commercial airlines to measure *in-situ*  $\text{CO}_2$

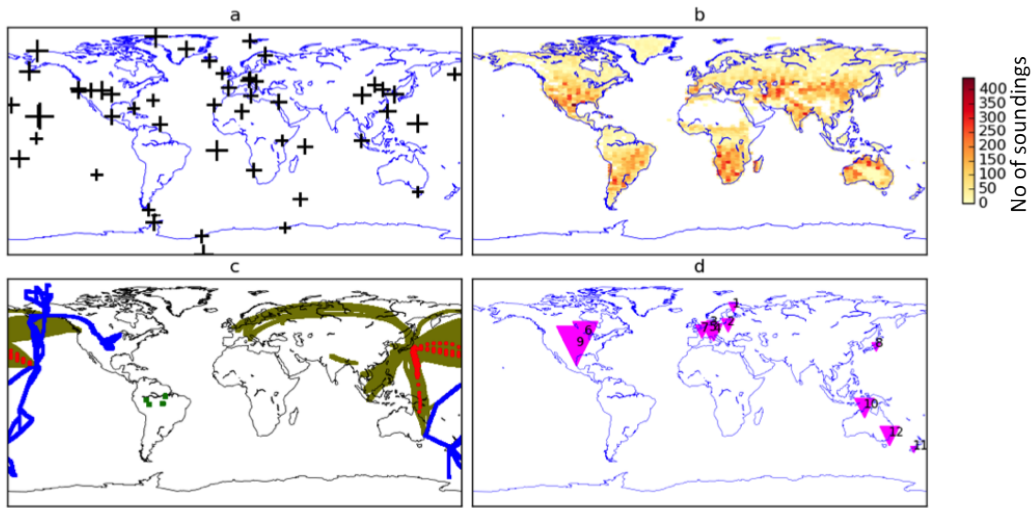


**Figure 1.** Measurements used in this study. a) The crosses indicate the locations of NOAA/ESRL surface sampling sites. The lengths of the vertical and horizontal bars are proportional to the number of CO<sub>2</sub> and CH<sub>4</sub> measurements, respectively. b) The number of GOSAT soundings binned at 1° × 1° for the time period of June 2009 to December 2010; c) Flight tracks of the aircraft campaigns HIPPO 2 and 3 (blue), CONTRAIL CO<sub>2</sub> (olive), CONTRAIL CH<sub>4</sub> (red), and AMAZONICA (green); d) The locations of the TCCON measurement sites. The numbers (1- 12) refer to corresponding entries in Table 1. The size of the purple rectangles is proportional to the number of collocated high-gain GOSAT soundings

by continuous measurement equipment (Machida et al., 2008). For some of the CONTRAIL flights CH<sub>4</sub> measurements are also available from flask-air samples. We use data from a lower-troposphere greenhouse-gas sampling program as part of the AMAZONICA project, over the Amazon Basin in 2010, measuring bi-weekly vertical profiles of CO<sub>2</sub> and CH<sub>4</sub> from above the forest canopy to 4.4 km above sea level at four locations: Tabatinga (TAB), RioBranco (RBA), Alta Floresta (ALF), and Santarem (SAN) (Gatti et al., 2014). The coverage of all aircraft measurements that were used in this study is shown in Figure 1.

### 2.3 Inversion Experiments

The following inversions have been performed:

1. SURF: Inversions assimilating flask air measurements of CH<sub>4</sub> or CO<sub>2</sub> to constrain surface fluxes of CH<sub>4</sub> or CO<sub>2</sub>, respectively.
2. RATIO: Inversion assimilating  $X_{\text{ratio}}$  and flask air measurements of CH<sub>4</sub> and CO<sub>2</sub> to constrain surface fluxes of CH<sub>4</sub> and CO<sub>2</sub>.
3. PR-MA: Inversion assimilating proxy  $XCH_4^{\text{ma}}$  and flask air measurements of CH<sub>4</sub> to constrain surface fluxes of CH<sub>4</sub>.



4. PR-CT: Inversion assimilating proxy  $XCH_4^{ct}$  and flask air measurements of  $CH_4$  to constrain surface fluxes of  $CH_4$ .

To assess the relative performance of each inversion, we validate atmospheric concentrations as simulated using the optimized fluxes from the different inversions with aircraft measurements. We define a normalized (i.e., divided by  $n$ ) chi-square statistic to quantify the agreement between the optimized model and aircraft measurements.

$$\kappa = \frac{1}{n}(\mathbf{y} - \mathbf{H}\mathbf{x})^T \mathbf{R}^{-1}(\mathbf{y} - \mathbf{H}\mathbf{x}), \quad (3)$$

Where  $\mathbf{y}$  is a vector of the aircraft measurements,  $n$  is the length of  $\mathbf{y}$ .  $\mathbf{H}\mathbf{x}$  is the TM5 simulation sampled at the measurement coordinates. The covariance matrix  $\mathbf{R}$  represents the expected uncertainty in the model–data mismatch. Its diagonal elements are calculated as the sum of the model representation error of TM5 and the measurement uncertainty; all non-diagonal elements are zero.

## 3 Results

### 3.1 ~~GOSAT-TCCON~~ GOSAT-TCCON comparison

TCCON measurements are used to investigate the errors in GOSAT-retrieved  $XCH_4$ . Each term on the right hand side of equation 2 contributes to the uncertainty in  $XCH_4^{proxy}$ . To quantify these error contributions, we compare TCCON measurements of  $X_{ratio}$ ,  $XCH_4$  and  $XCO_2$  to corresponding co-located GOSAT-retrievals. The validation is carried out for the time period of 1st June 2009 to 31st December 2013, for which both proxy datasets ( $XCH_4^{ma}$  and  $XCH_4^{ct}$ ) are available. Table 1 shows mean differences per TCCON station, expressed as fractional differences to facilitate the comparison of quantities with different units. As expected, the largest differences between GOSAT and TCCON are found for  $XCO_2^{ns}$  and  $XCH_4^{ns}$ . In general,  $XCO_2^{ns}$  (mean = -1.57%) shows larger relative differences than  $XCH_4^{ns}$  (mean = -0.95%). A latitudinal dependence can be observed, with increasing biases towards stations at higher latitudes. This can be explained by increased aerosol scattering at larger sun angles, as the light path through the atmosphere is longer. For all the stations, the mean difference is negative which is expected for aerosol scattering-induced errors at the low surface albedos of the TCCON sites (Houweling et al., 2004). The smaller bias values for  $X_{ratio}$  than  $XCO_2^{ns}$  and  $XCH_4^{ns}$  confirm that scattering-induced errors cancel out in the ratio, which motivated the proxy approach (Frankenberg et al., 2005). Overall, we observe that  $X_{ratio}$  (mean bias = 0.59 %) is the **dominant** larger contributor to the error in  $XCH_4^{proxy}$  ~~-than~~ than MACC ( $XCO_2^{ma}$ , mean bias = 0.01%) and CarbonTracker ( $XCO_2^{ct}$ , mean bias = 0.24%) ~~contribute relatively less errors~~.

### 3.2 Inversion results

#### 3.2.1 Assimilation statistics

Figure 2 summarizes the statistics of the model – measurement comparison. The prior  $X_{ratio}$  mismatches typically fall in the range ~~-1 to +1~~  $\pm 1$  % (with mean = 0.007 ppb/ppm and  $1\sigma = 0.043$  ppb/ppm). The inversions reduce the average mismatch by



**Table 1.** TCCON validation of the components of  $XCH_4^{proxy}$  (see Equation 2). The numbers represent mean percentage differences with TCCON (weighted with TCCON + GOSAT error). A negative number means that the satellite retrieval is lower than TCCON. Data from these stations was used: Sodankyla (Kivi et al., 2014), Bialystok Deutscher et al. (2014a), Bremen (Deutscher et al., 2014b), Garmisch (Sussmann and Rettinger, 2014), Karlsruhe (Hase et al., 2014), Parkfalls (Wennberg et al., 2014a), Orleans (Warneke et al., 2014), Tsukuba (Morino et al., 2014), Lamont (Wennberg et al., 2014b), Darwin (Griffith et al., 2014a), Lauder (Sherlock et al., 2014), Wollongong (Griffith et al., 2014b) are arranged from north to south. (for TCCON site locations see Figure 1).

Station	No. of collocated measurements	Mean differences with TCCON ( % )				
		XCO <sub>2</sub> <sup>ns</sup>	XCH <sub>4</sub> <sup>ns</sup>	X <sub>ratio</sub>	XCO <sub>2</sub> <sup>ct</sup>	XCO <sub>2</sub> <sup>ma</sup>
Sodankyla	434	-3.03	-2.81	0.21	0.68	0.34
Bialystok	731	-2.46	-1.79	0.62	0.31	0.05
Bremen	426	-1.81	-0.99	0.76	-0.05	-0.32
Garmisch	1295	-1.93	-1.09	0.76	0.40	0.05
Karlsruhe	1244	-1.74	-1.00	0.69	0.15	-0.25
Parkfalls	2174	-1.23	-0.43	0.75	0.22	0.11
Orleans	808	-1.53	-0.75	0.75	0.21	-0.09
Tsukuba	135	-1.87	-1.24	0.63	0.57	-0.03
Lamont	5617	-0.73	-0.03	0.68	0.07	-0.00
Darwin	1065	-0.67	-0.19	0.47	0.02	0.14
Lauder	110	-1.05	-0.57	0.46	0.14	0.03
Wollongong	1515	-0.81	-0.45	0.35	0.10	0.00

about a factor of 10, and the variation of single column mismatches by about a factor of 2. The  $XCH_4^{proxy}$  of PR-CT and PR-MA have bimodal prior mismatches, because the *a priori* model overestimates the north-south gradient of CH<sub>4</sub>. The bottom panels of Figure 2 show mismatches between TM5 and surface flask measurements of CH<sub>4</sub> and CO<sub>2</sub>. The CH<sub>4</sub> *a priori* measurement mismatch has a mean of -18.30 ppb and a 1  $\sigma$  of 42.30 ppb. The RATIO, SURF, PR-CT, and PR-MA inversions are all able to

5 fit the NOAA data to a similar extent, reducing the *a priori* differences by more than a factor of 20. CO<sub>2</sub> flask measurements are assimilated in SURF and RATIO. Both inversions reduce the *a priori* mismatch (mean = -2.12 ppm, 1  $\sigma$  = 3.88 ppm), with RATIO (mean = -0.04 ppm, 1  $\sigma$  = 3.69 ppm) fitting the CO<sub>2</sub> flask data as well as SURF (mean = -0.06 ppm, 1  $\sigma$  = 3.72 ppm).

### 3.2.2 CH<sub>4</sub> fluxes

Optimized annual CH<sub>4</sub> fluxes, integrated over the TRANSCOM regions are shown in the left panel of Figure 3. The fluxes

10 obtained with the RATIO inversion are on average more similar to fluxes from other GOSAT inversions than to the surface inversion, with a few exceptions. Differences between satellite and surface inversion are most prominent over Tropical South America, where the latter is closer to the prior, which can likely be explained by the lack of surface measurement coverage.

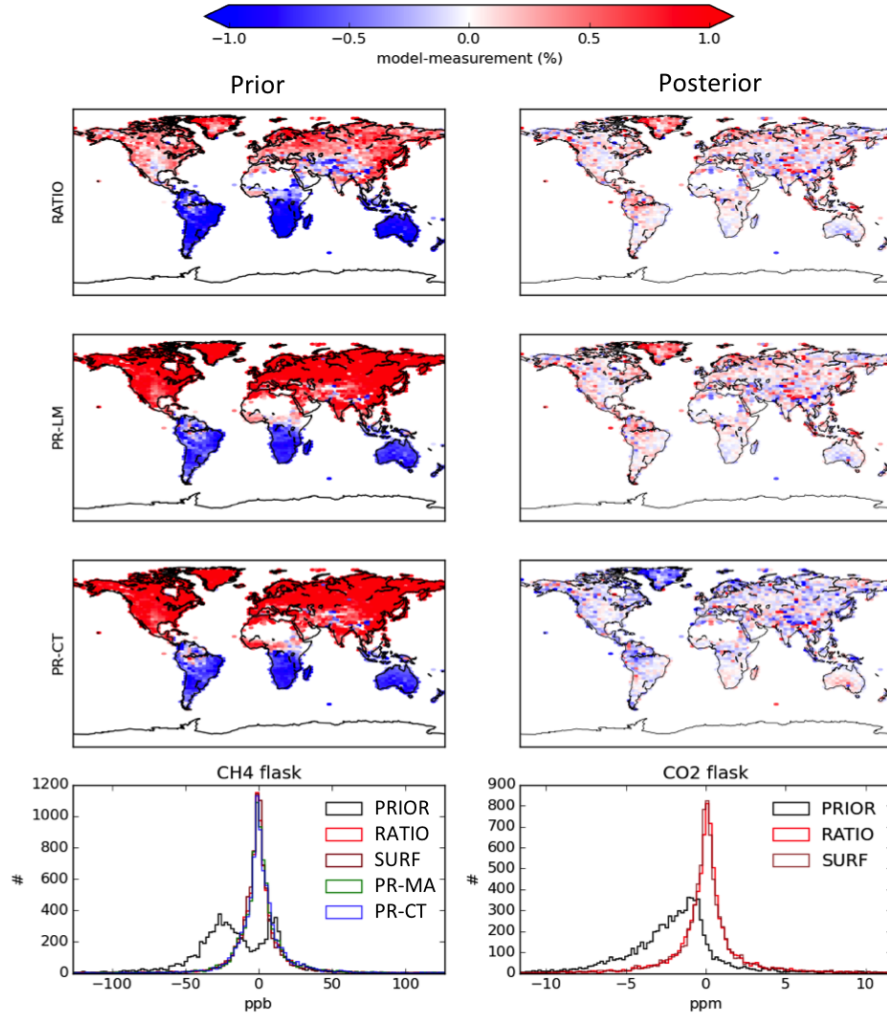


**Figure 2.** Fit residuals, comparing the performance of different inversions. The top three rows show the difference between TM5-4DVAR and GOSAT measurements ( $X_{\text{ratio}}$  for RATIO,  $X\text{CH}_4^{\text{proxy}}$  for PR-CT and PR-MA), using *a priori* (left) and *a posteriori* (right) fluxes. The bottom row shows histograms of measurement–model mismatches between TM5-4DVAR and NOAA surface measurements in 400 bins between  $\pm 10 \sigma$  range of the *a priori* mismatch.

We will return to the inversion results for Tropical South America in section 3.2.6, where validation results are shown using aircraft data.

The most significant difference between the satellite inversion and SURF is found for Temperate Eurasia, where SURF reduces the  $\text{CH}_4$  emissions from 121 Tg/y in the prior estimate to 66 Tg/y. When satellite data are added, the fluxes increase again

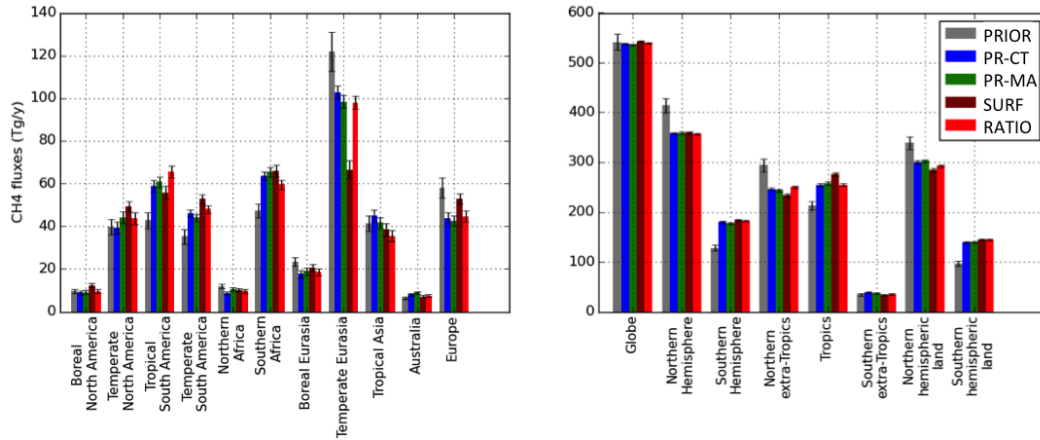


**Figure 3.** Annual fluxes of  $\text{CH}_4$  integrated over different regions. The black line on each bar represents the  $\pm 1 \sigma$  uncertainty.

to 100 Tg/y in the region. The large flux correction in the SURF inversion is compensated by increases in other TRANSCOM regions of 5-10 Tg/y (see for example Temperate North and South America). In those regions satellite inversions remain closer to the prior than the SURF inversion, which may well be driven by the much smaller flux corrections for Temperate Eurasia.

- 5 The exception is Europe, where the satellite inversions show larger reductions of up to 15 Tg/y. The large adjustments over Temperate Eurasia are analyzed further in section 3.2.7. PR-CT and PR-MA result in relatively similar posterior annual fluxes for all regions. RATIO is in good agreement with the proxy inversions except for Tropical South America and Southern Africa. The right panel of Figure 3 shows annual fluxes integrated over large regions on the globe. We find a consistent adjustment in the north-south gradient of  $\text{CH}_4$  compared to the prior in all inversions, corresponding to an emission shift from the Northern
- 10 to the Southern Hemisphere of approximately 50 Tg/y. This might be due to an overestimation of the *a priori* emissions from northern wetlands, as discussed in (Spahni et al., 2011). A bias in inter-hemispheric transport in TM5 is not a likely cause, since the use of ECMWF archived convective fluxes in TM5 has been shown to lead to a realistic simulation of the north-south gradient of  $\text{SF}_6$  (Vanderlaan et al., 2015). Houweling et al. (2014) found similar  $\text{CH}_4$  emission shifts between the hemispheres, after bringing the inter-hemispheric transport in agreement with  $\text{SF}_6$  using a parameterization of horizontal diffusion.

- 15 Next we shift focus to seasonal differences between the inversion-derived methane fluxes (see Figure 4). Also on the seasonal scale, RATIO resembles the two PROXY inversions more than SURF. In Boreal North America, the satellite inversions that assimilate GOSAT soundings are in better agreement with the prior. We observe an increase in summertime  $\text{CH}_4$  fluxes in SURF estimates for Boreal and Temperate North America. The differences in annual mean fluxes discussed earlier for Tropical South America and Temperate Eurasia do not show ~~an important a~~ seasonal dependence. Large differences in seasonality are
- 20 obtained for Australia and the African regions, which also show important differences between the two proxy inversions (see Section 3.2.4). In Southern Africa, all inversions show increased  $\text{CH}_4$  fluxes compared to the prior estimate; however, small differences can be seen between the two proxy inversions, especially in 2010. SURF remains in good agreement with PRIOR, which is expected as no surface observations are available to constrain the fluxes in this region.

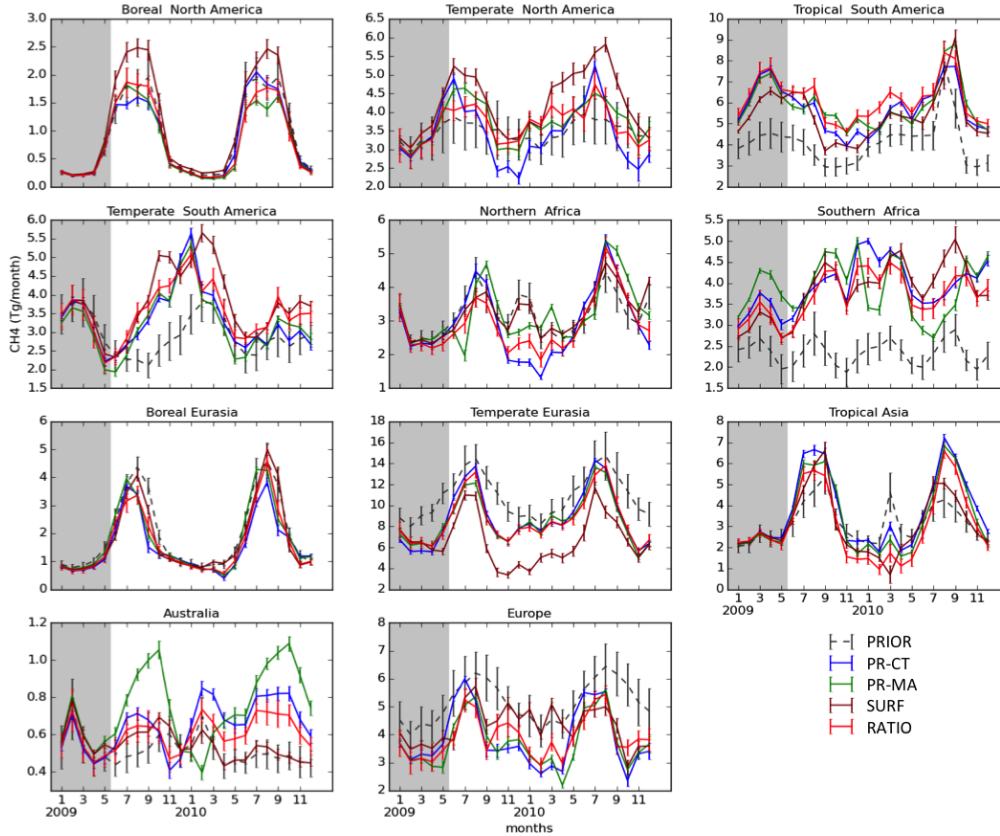


**Figure 4.** Monthly fluxes of  $\text{CH}_4$  integrated over TRANSCOM regions. The vertical lines represent a  $1\sigma$  uncertainty of the monthly fluxes. The gray region in each plot represents the period in which no measurements are assimilated.

### 3.2.3 $\text{CO}_2$ fluxes

Annual  $\text{CO}_2$  fluxes from the SURF and RATIO inversions, integrated over TRANSCOM regions, are shown in Figure 5. Overall, we find good consistency between the results from RATIO and SURF except for Temperate Eurasia, where RATIO results in a higher  $\text{CO}_2$  uptake of  $0.5 \text{ PgC/y}$ . Corresponding reductions in  $\text{CH}_4$  fluxes are found for this region in the RATIO inversion. This can be understood by realizing that the satellite information  $\bar{\gamma}$  that is used  $\bar{\gamma}$  consists of the ratio of  $\text{CH}_4$  and  $\text{CO}_2$  columns. A RATIO inversion can simultaneously reduce the  $\text{CO}_2$  and  $\text{CH}_4$  fluxes over a region without changing the  $X_{\text{ratio}}$  in the atmosphere. SURF points towards a natural sink of  $0.5 \text{ PgC/y}$  in Boreal North America. RATIO and the *a priori* are carbon neutral in this region. This agreement is also seen on the  $\text{CH}_4$  side of the RATIO inversion. Only small differences between the posterior and prior fluxes of SURF and RATIO are found over the oceans except for the Temperate North Pacific, which is neutral in both inversions compared to a sink of  $-0.5 \text{ PgC/y}$  in the prior fluxes, and in Tropical India which is turned into a net sink. Interestingly, RATIO leads to posterior fluxes for Europe that are close to carbon neutral for the analysis period. This is in

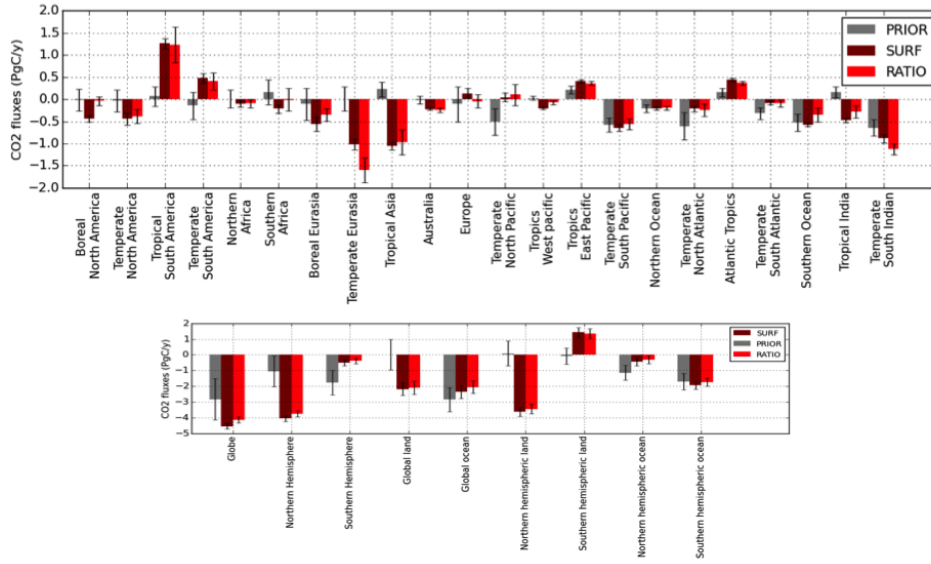


**Figure 5.** Annual fluxes of CO<sub>2</sub> (excluding fossil fuel emissions) integrated over different regions.

contrast with the findings of several inversions using GOSAT full physics XCO<sub>2</sub> retrievals, suggesting a largely underestimated European carbon sink of the order of 1 PgC/y (Basu et al., 2014; Chevallier et al., 2014; Reuter et al., 2014; Houweling et al., 2015).

- 5 The RATIO and SURF inversions increase the global CO<sub>2</sub> sink of the terrestrial biosphere compared with the *a priori* fluxes. This is primarily caused by the bottom-up CASA model, which has been reported to underestimate the carbon uptake of the Northern biosphere sink in summer season (Yang et al., 2007). Basu et al. (2013) also find a global natural sink of 3 to 4 PgC/y for GOSAT and NOAA inversions. This natural sink is needed to fit the atmospheric growth rate of CO<sub>2</sub> in the presence of about 9 PgC/yr anthropogenic emissions. The Southern Hemisphere land is turned into a source of 1 PgC/y in both inversions.

#### 10 3.2.4 Errors in CO<sub>2</sub><sup>model</sup>

- In this Section, we analyze the differences between the two proxy retrievals (XCH<sub>4</sub><sup>ct</sup> and XCH<sub>4</sub><sup>ma</sup>) and how they propagate into posterior CH<sub>4</sub> fluxes. Note that these differences arise only from differences in XCO<sub>2</sub><sup>model</sup>, and therefore large differences between the XCH<sub>4</sub><sup>proxy</sup> measurements point towards high uncertainties in the model representations of atmospheric CO<sub>2</sub>. Figure 6 further displays the result of these inversions. We find a mean difference between XCH<sub>4</sub><sup>ma</sup> and XCH<sub>4</sub><sup>ct</sup> of -2.36 ppb and a  $\sigma$  of 4.55 ppb. This is caused by mean differences between XCO<sub>2</sub><sup>ma</sup> and XCO<sub>2</sub><sup>ct</sup> of -0.50 ppm and a  $\sigma$  of 0.97 ppm (not shown in the Figure). We find a seasonal variation in the difference with the largest amplitudes of about 10 ppb in the northern tropics. The phasing varies with latitude, with positive values during boreal summer to autumn. The smallest differences are found in the Southern Hemisphere. The bottom panel of Figure 6 shows how this seasonal pattern propagates into the posterior CH<sub>4</sub>

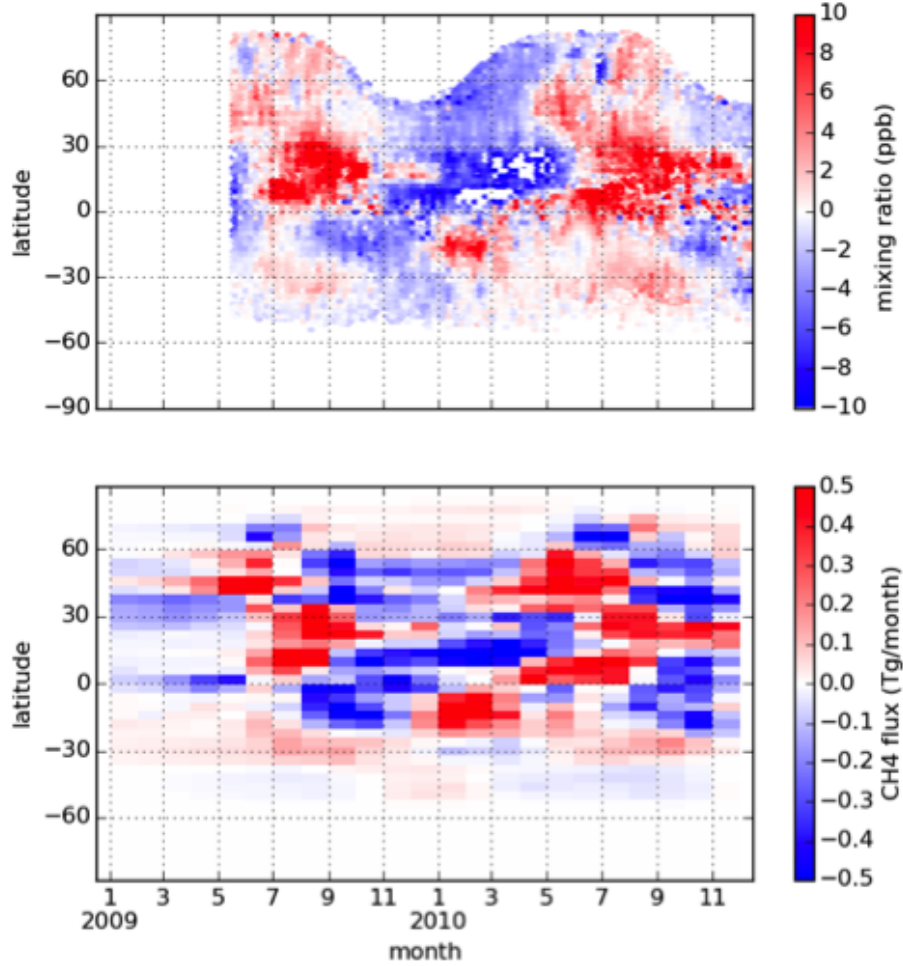


**Figure 6.** Top: Zonally averaged differences in CH<sub>4</sub> column mixing ratio between the two XCH<sub>4</sub><sup>proxy</sup> retrievals (XCH<sub>4</sub><sup>ma</sup> - XCH<sub>4</sub><sup>ct</sup>). Bottom: Corresponding differences in *a posteriori* CH<sub>4</sub> flux between the proxy inversions using these data (PR-MA minus PR-CT).

fluxes. The seasonal and latitudinal variation in the CH<sub>4</sub> flux difference follows the variation in the XCH<sub>4</sub><sup>proxy</sup> difference, with an amplitude of 0.5 Tg/month/gridcell. The regions without satellite data coverage, i.e. below 60° S and above 60° N, show smaller differences in the optimized fluxes.

- 5 PR-CT and PR-MA yield different CH<sub>4</sub> fluxes in Northern Africa and Australia (see Figure 4). We plot these fluxes with the corresponding regional averaged XCH<sub>4</sub> values in Figure 7. For Northern Africa, the difference in XCH<sub>4</sub><sup>proxy</sup> of up to 10 ppb around January 2010 gives rise to a difference in the monthly posterior flux of 1 Tg/month. In Australia, XCH<sub>4</sub><sup>ma</sup> and XCH<sub>4</sub><sup>ct</sup> are in relatively good agreement with each other, with differences within 2 ppb. However, because the *a priori* emission



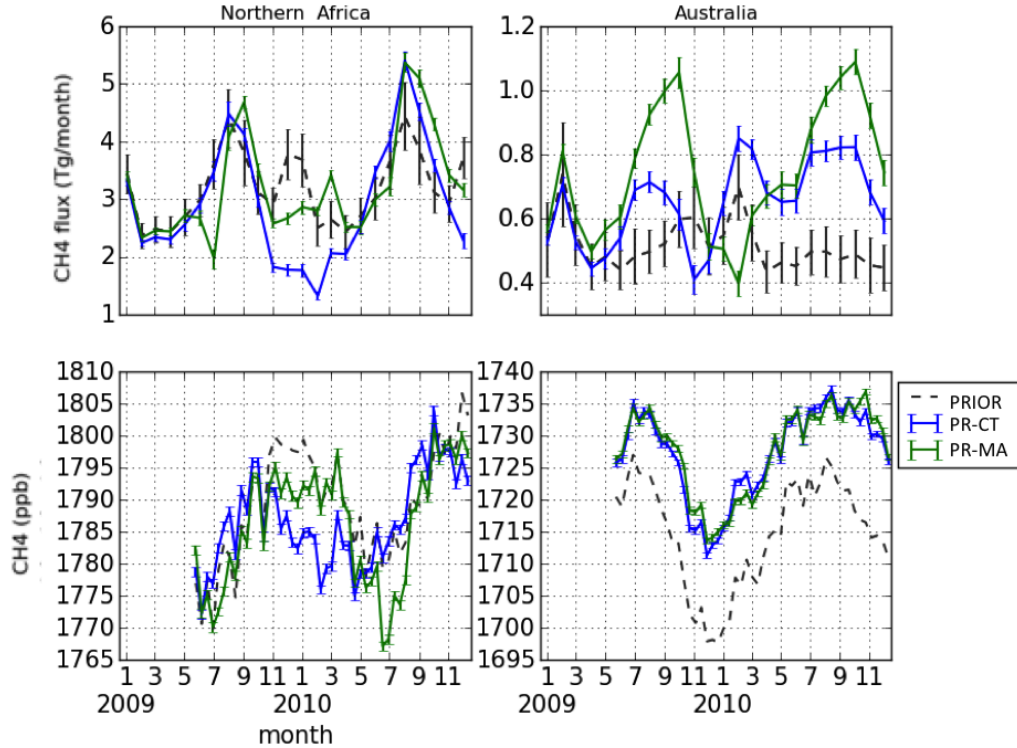


**Figure 7.** The top panels shows the posterior monthly fluxes integrated over TRANSCOM region. Bottom panels show the time series of the mean of  $XCH_4^{proxy}$  over Northern Africa and Australia. The dotted line in the bottom panels denotes the mean of *a priori* modeled  $XCH_4$  sampled at GOSAT sites.

from this region is very small, the difference in the optimized seasonal cycle of fluxes nevertheless becomes relatively large. In particular PR-MA causes significant deviations from the *a priori*, with decreases in the posterior fluxes during Australian summer, and large increases during winter. Another reason for these flux adjustments is the limited land area in the Southern Hemisphere that is available for  $CH_4$  flux adjustments (over the open ocean the *a priori* flux uncertainties are small limiting their adjustment).

(Detmers et al., 2015) reported an enhanced  $CO_2$  sink over Central Australia in the second half of 2010 lasting until 2012, caused by an increase in vegetation due to enhanced precipitation during *La-Nina* conditions. If not properly represented in inversions using surface measurements, this negative  $CO_2$  anomaly causes  $XCO_2^{model}$  to be overestimated. In that case, the anomaly propagates to the proxy retrievals resulting in overestimation of  $XCH_4^{proxy}$ , leading to overestimated *a posteriori*  $CH_4$  fluxes. RATIO estimates a significantly stronger sink of  $CO_2$  in agreement with (Basu et al., 2013) (see supplementary Figure 2). This results in lower  $CH_4$  fluxes in the RATIO inversion (see Figure 4), demonstrating how the RATIO inversion method can avoid shortcomings in the proxy inversions in regions where  $CO_2$  is poorly constrained by surface data.

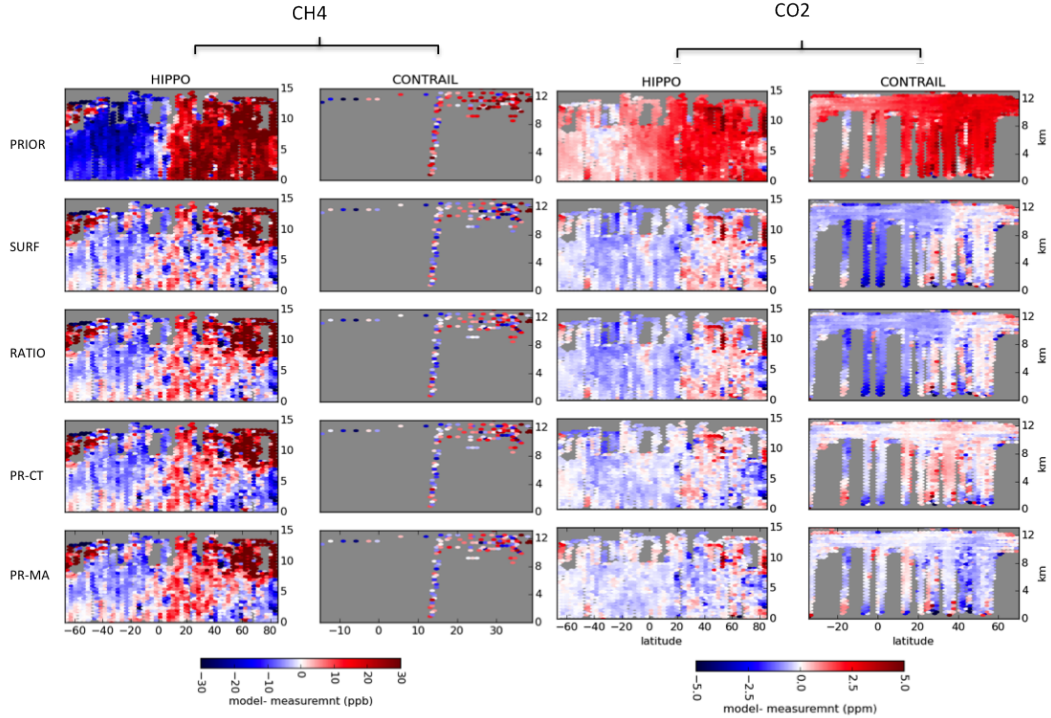


**Figure 8.** Validation of inversion-optimized concentration fields of  $\text{CO}_2$  and  $\text{CH}_4$  with air-borne measurements.

PR-CT and PR-MA have opposite seasonal cycles, which may be due to their  $\text{XCO}_2^{\text{model}}$  components, which are derived using different ecosystem models. Carbontracker uses *a priori* natural fluxes from a CASA simulation driven by actual climatological information, whereas MACC uses only the climatology of natural fluxes. Therefore, the inter-annual variability of the inverted

5 fluxes in MACC is driven by measurements only. Since the surface network does not pose strong constraints on the Australian carbon budget, the differences are driven by the prior fluxes of the two models, which may be more realistic in Carbontracker in this case.

### 3.2.5 Aircraft Validation

To further investigate the performance of our inversions, we validate the inversion-optimized  $\text{CH}_4$  and  $\text{CO}_2$  mixing ratios

10 against independent aircraft measurements obtained during the projects described in section 2.2. The results of the HIPPO and CONTRAIL validation are shown in figure 8 and the values for  $\kappa$  for  $\text{CH}_4$  and the root mean square difference (RMSD) for  $\text{CO}_2$  are given in 9.  $\kappa$  values are not calculated for  $\text{CO}_2$  because we do not have the  $\text{CO}_2$  model representation errors used in MACC and CarbonTracker. More details on statistics of the validation are provided in Table 1.

The difference between HIPPO and PRIOR reflects the overestimated north-south gradient that is found using *a priori*  $\text{CH}_4$  fluxes, as already discussed in section 3.2.2. In addition, PRIOR shows a uniform bias of 13.5 ppb. SURF and RATIO correct



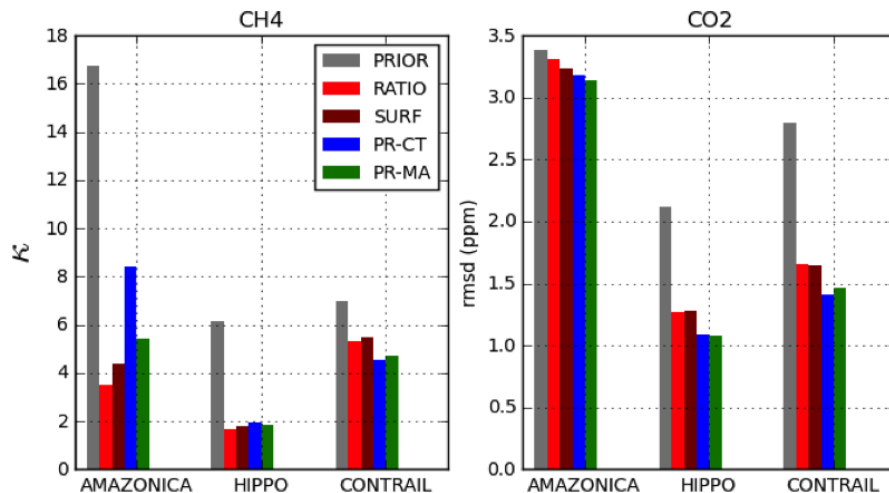


**Figure 9.** Summary of aircraft validation results per project for CH<sub>4</sub> (left panel, expressed as  $\kappa$ ) and CO<sub>2</sub> (right panel, expressed as RMSD) for the whole inversion time period i.e. from 1/1/2009 to 31/12/2010.

the north-south gradient and reduce biases to 5.56 and 6.68 ppb, respectively. All the models are performing equally well in terms of  $\kappa$ . The original MACC and CarbonTracker CO<sub>2</sub> fields have RMSD values of 1.08 and 1.09 ppm, respectively, which is lower than the RMSD of RATIO (1.64 ppm) and SURF (1.65 ppm). We suggest that CarbonTracker and MACC have a better representation of CO<sub>2</sub> than PR-CT, PR-MA and SURF as they assimilate a larger number of flask measurements sites and also few continuous *in-situ* sites.

Compared with the large CONTRAIL dataset of CO<sub>2</sub> measurements, only a limited number of CH<sub>4</sub> measurements are available, mostly over the Pacific Ocean (see Figure 1). We observe the same north-south gradient mismatch with PRIOR as seen in the comparison to HIPPO. PR-CT is able to improve the PRIOR  $\kappa$  of 6.99 to 4.56, followed in order of decreasing performance by PR-MA (4.71), SURF (5.33), and RATIO (5.47). The values of  $\kappa$  are larger than 1, which points to significant errors in all the inversion results. The RMSD of the different inversions are comparable. The large dataset of CONTRAIL CO<sub>2</sub> measurements covers a much larger area, including flight tracks to Europe and South East Asia. Our validation shows a mean error of 2.23 ppm in PRIOR. The NOAA and RATIO inversions reduce this bias to -0.43 ppm and -0.41 ppm, respectively. However, similar to the HIPPO validation, MACC (mean bias = -0.2 ppm) and CarbonTracker-derived CO<sub>2</sub> (mean bias = 0.11 ppm) fields are in better agreement with the CONTRAIL measurements than the other inversions.

### 3.2.6 Tropical South America

Tropical South America contains the Amazon basin, which is a large reservoir of standing biomass and contains one of the largest wetlands in the world. Therefore, it plays an important role in the annual global budget of both CO<sub>2</sub> and CH<sub>4</sub>. Inversion results for the region have been validated using AMAZONICA measurements (see Supplementary Figure 5 and Supplementary

Table 1). Generally, the model results using PRIOR emissions underestimate the measured CH<sub>4</sub> mixing ratios (mean offset=-32.02 ppb). All inversions correct this offset, with SURF performing best (mean offset=-14.18 ppb). RATIO closely follows SURF with a mean mismatch of -17.18 ppb. The proxy inversions have a higher mismatch than RATIO and SURF, with means of -20.30 and -24.11 ppb respectively for PR-MA and PR-CT. The  $\kappa$  values for the AMAZONICA CH<sub>4</sub> measurements (see Figure 9) again show that fluxes from RATIO lead to lower mismatches than those from PR-CT and PR-MA. RATIO predicts this region as a significantly high CH<sub>4</sub> source for the first half of 2010 (see Figure 4), and is in good agreement with aircraft measurements.

To check whether this is caused by errors in  $XCO_2^{\text{model}}$ , we perform similar comparisons using AMAZONICA CO<sub>2</sub> measurements. We find that the two original models represent CO<sub>2</sub> about equally well in terms of RMSD (see Supplementary Table 1). Therefore, the ~~lesser performance~~ higher mismatch of PR-CT and PR-MA for CH<sub>4</sub> is not due to a poor representation of the  $XCO_2^{\text{model}}$  over the region. This raises the question why RATIO performs better? In sections 3.1, we observe that the error in  $CO_2^{\text{model}}$  is generally lower than the error in the GOSAT  $X_{\text{ratio}}$  retrievals (see section 3.1. In proxy inversions, this retrieval error, which is coming from  $X_{\text{ratio}}$  (see equation 2), is directly transferred to CH<sub>4</sub> fluxes, whereas in RATIO it is distributed over the CH<sub>4</sub> and CO<sub>2</sub> part of the state vector. The high posterior CO<sub>2</sub> flux uncertainties for RATIO in the region support this further (see Figure 5).

Flux maps of the region show that the satellite inversions provide a more spatially resolved adjustment of the CH<sub>4</sub> fluxes than SURF (see Supplementary Figure 3). The satellite inversions estimate higher fluxes in the northwest corner of the region near Columbia. Similar increases have been reported in earlier studies assimilating satellite retrieved XCH<sub>4</sub> (Monteil et al., 2013; Frankenberg et al., 2006). The spatial pattern of the flux adjustment suggests that the proxy inversions compensate the increase over Columbia by reducing the fluxes in the Amazon Basin, which is less well covered by satellite retrievals due to frequent cloud cover. This may explain why the proxy inversions end up underestimating the observations inside the Basin. SURF is mainly constrained by the large-scale inter-hemispheric gradient. This leads to a different pattern of flux adjustments, increasing only the fluxes in the southern part of the region while keeping the fluxes in Amazon Basin close to the prior. This solution brings SURF in relatively close agreement with the measurements. RATIO also shows a flux enhancement in Columbia, but at the same time represents the Amazon Basin better than the proxy inversions, likely because of its larger number of degrees of freedom in modifying regional flux patterns of both CO<sub>2</sub> and CH<sub>4</sub>.

Gatti et al. (2014) and Vanderlaan et al. (2015) reported an anomalous natural source of CO<sub>2</sub> in the region in 2010, also using AMAZONICA aircraft measurements. In this study, RATIO predicts a more enhanced CO<sub>2</sub> natural source than the SURF and PRIOR. RATIO (RMSD=3.23 ppm) is also in better agreement in terms of RMSD with AMAZONICA CO<sub>2</sub> data than SURF (RMSD=3.31 ppm) and PRIOR (3.38 ppm). This demonstrates, like in the case of Australia, that the RATIO method is capable of informing us about the CO<sub>2</sub> fluxes, from which the CH<sub>4</sub> flux estimation benefits also.

### 3.2.7 Temperate Eurasia

As mentioned in section 3.2.2, SURF leads to a drastic emission reduction in Temperate Eurasia, whereas all satellite inversions show comparatively smaller decreases. Here, we investigate this in further detail by analyzing the inversion-optimized fits to

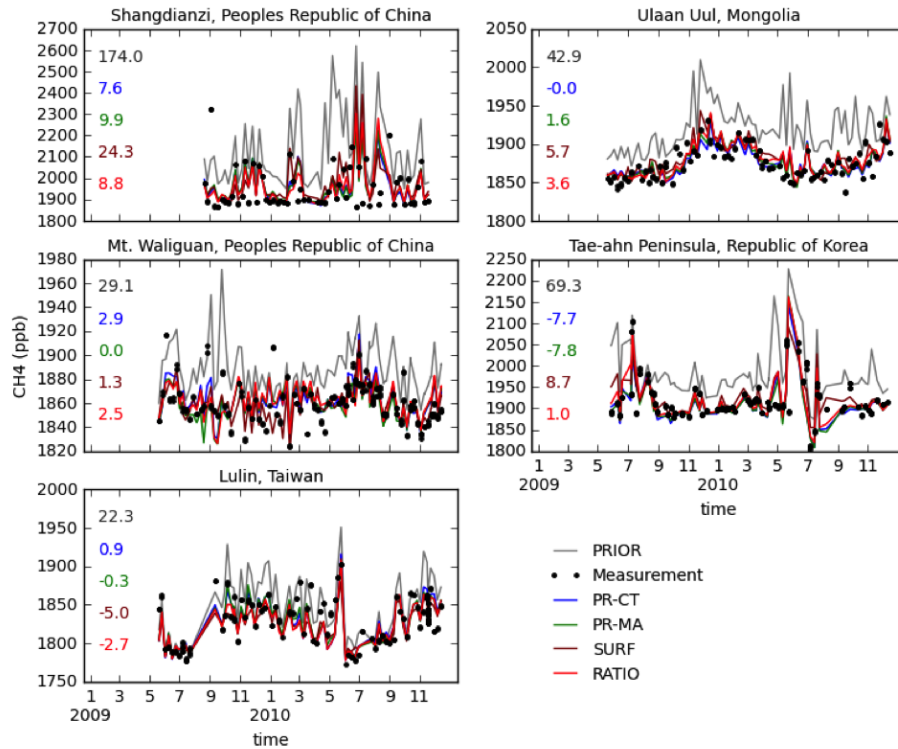


**Figure 10.** Inversion-optimized fits to surface measurement sites in Temperate Eurasia. The numbers in the plots are the mean bias of models with measurements.

the NOAA measurements at five surface sites located in this region (Figure 10). We find large mismatches between the *a priori* simulated concentrations and the measurement at these sites, with mean offsets ranging between 29.1 ppb at Mt. Waliguan and 174 ppb at Shangdianzi. All inversions correct for this mismatch by decreasing the regional emissions. Surprisingly enough, the satellite inversions are able to fit the flask measurements even better than SURF, despite smaller corrections to the fluxes. For example, the mean posterior mismatch at Shangdianzi is 24.3 ppb for SURF, and only 7.5 ppb to 9.8 ppb for the satellite inversions. A possible explanation is the double counting of surface data in the satellite inversions, because the satellite data have been bias corrected using an inversion that was already optimized using surface data. However, the bias correction is only applied as a zonal and annual mean. All inversions show similar reductions in the fluxes from eastern Temperate Eurasia (mostly China) to match the NOAA measurements. However, the satellite inversions tend to compensate for this flux decrease over China by increased fluxes in India and the central part of Temperate Eurasia.

## 4 Discussion

We have demonstrated that the application of the ratio method to GOSAT data yields realistic solutions for CO<sub>2</sub> and CH<sub>4</sub> fluxes. Its performance is comparable, and may in some regions even be better than the proxy inversion method. This is an important finding because the X<sub>ratio</sub> retrieval approach provides a useful alternative to the full-physics method in that cloud filtering is less critical. In the case of GOSAT, it increases the number of useful measurements by about a factor of two (Butz et al., 2010; Fraser et al., 2014). At the same time, the RATIO inversion method avoids using the model-derived-CO<sub>2</sub> fields as a hard constraint, which is the an important limitation of the proxy method.

The realistic performance of the ratio method is certainly not a trivial outcome, since it prompts the user for specification of new uncertainties influencing the way in which measurement information is shared between CH<sub>4</sub> and CO<sub>2</sub>. The joint CO<sub>2</sub> and CH<sub>4</sub> inversion problem has a larger number of degrees of freedom, as a result of which CH<sub>4</sub> flux adjustments can compensate for errors in CO<sub>2</sub> and vice versa. Assimilating surface measurements helps decoupling CH<sub>4</sub> and CO<sub>2</sub>, which works best in regions that are relatively well covered by the surface network.

In other regions, the method can be improved further by accounting for correlations between *a priori* fluxes of CH<sub>4</sub> and CO<sub>2</sub>. This study does not specify such correlations, which corresponds to the assumption that *a priori* CO<sub>2</sub> and CH<sub>4</sub> flux uncertainties are independent of each other. Fraser et al. (2014) accounted for *a priori* uncertainty correlations for biomass burning fluxes of CO<sub>2</sub> and CH<sub>4</sub>, based on the available information about emission ratios. Imposing such *a priori* constraints increased posterior uncertainty reduction compared to other methods for both CH<sub>4</sub> and CO<sub>2</sub> in some regions.

It is noteworthy that the inversions are run assuming uncorrelated measurements and a perfect transport. Also, as we are not optimizing the atmospheric sink of CH<sub>4</sub>, all the information from its budget is used to constrain the surface fluxes. Hence, the estimates of posterior uncertainties tend to be optimistic in this study. The  $\chi^2$  statistic indicates whether the assumed measurement and prior errors are statistically consistent (Meirink et al., 2008). We find  $\chi^2/n_s = 0.93$  for RATIO, 0.96 for PR-CT, 0.93 for PR-LM and 1.14 for SURF in the CH<sub>4</sub> inversions ( $n_s$  is the number of observations assimilated in the inversion). This shows that we are not drastically underestimating the prior uncertainties in our CH<sub>4</sub> inversions.

One problem with the ratio method is the assimilation of X<sub>ratio</sub> over oceans. The uncertainty of CH<sub>4</sub> fluxes over the open oceans is relatively small. As a result, the model-data mismatch over the ocean is mostly accounted for by adjusting the CO<sub>2</sub> fluxes, which has a larger *a priori* uncertainty. At the same time, CO<sub>2</sub> fluxes over oceans tend to be very sensitive to small and systematic model-data mismatches of a few tenths of a ppm (Basu et al., 2013). Any bias in atmospheric transport, affecting both CO<sub>2</sub> and CH<sub>4</sub> is projected on the CO<sub>2</sub> fluxes, which may lead to rather unrealistic estimates of the annual CO<sub>2</sub> exchange over oceanic regions. Palmer et al. (2006) proposed to account for cross correlations in the model representation error between the components of a dual tracer inversion, which could reduce this problem.

Our surface-only inversion shows a large decrease in the fluxes from Temperature Eurasia. To better understand this, we look at results of other recently published CH<sub>4</sub> inversion results. We group the studies into three groups: 1. Studies not using EDGAR v4.2 as prior, comprising of Houweling et al. (2014); Monteil et al. (2013); Bruhwiler et al. (2014); Fraser et al. (2013); 2. Studies using EDGAR v4.2 but not assimilating the Shangdianzi site, comprising of Alexe et al. (2014); Bergamaschi et al.

(2013); 3. Studies using EDGAR v4.2 and assimilating Shangdianzi site comprising of this work and Thompson et al. (2015). The inversions of group 1 do not show a systematic reduction in fluxes of Temperate Eurasia. Inversions of Group 3 tend to reduce the emissions from the region the most, whereas, group 2 reduces emissions by an intermediate amount. This outcome is partly explained by the EDGAR 4.2 emissions being substantially higher in Temperate Eurasia than previous EDGAR versions, as found also by Bergamaschi et al. (2013). In addition, however, these increased emissions have the largest impact on surface-only inversions assimilating measurements from the Shangdianzi site, possibly due to a nearby hot spot in EDGAR v4.2. The hotspot is located near Jiexiu in the Shanxi province (112E, 37N), and has coal emissions of 10.83 Tg/yr for the year 2010 from a  $10 \times 10$  km grid. According to the EDGAR team (G. Meinhout, personal communication), this unrealistically high local source of  $\text{CH}_4$  is the consequence of disaggregating large emission from Chinese coal mining using the limited available information on the location of the coal mines. Thompson et al. (2015), the other study in group 3, show a large *a priori* mismatch with a root mean square error of 103 ppb at Shangdianzi. Their inversions reduce an *a priori* East Asian  $\text{CH}_4$  emission of 82 Tg/y by 23 Tg/y, with large adjustments in the emissions from rice cultivation. Further research is needed to investigate the implications of the shortcoming of EDGAR v4.2. It is noteworthy, however, that when satellite data are assimilated in these studies, the improved regional coverage reduces the impact of this local disaggregation problem on the estimated regional emissions.

## 5 Conclusions

This study investigated the use of GOSAT-retrieved- $X_{\text{ratio}}$  for constraining the surface fluxes of  $\text{CO}_2$  and  $\text{CH}_4$ . First, we validated the  $X\text{CH}_4$ ,  $X\text{CO}_2$  and  $X_{\text{ratio}}$  retrievals, as well as the model-derived- $X\text{CO}_2$  fields used in the proxy methods, using TCCON measurements. This analysis confirmed that biases in non-scattering  $X\text{CH}_4$  and  $X\text{CO}_2$  retrievals largely cancel out in  $X_{\text{ratio}}$ .  $X_{\text{ratio}}$  has a larger mean bias than model-derived- $X\text{CO}_2$  from CarbonTracker and MACC, suggesting that mostly retrieval biases, rather than  $\text{CO}_2$  model errors, limit the performance of the proxy method. This is true especially at large temporal and spatial scale. To account for biases in GOSAT-retrieved  $X_{\text{ratio}}$  a TCCON-derived correction was applied as a function of surface albedo, resulting in a mean adjustment of -0.74%. An additional correction was applied to  $X_{\text{ratio}}$ ,  $X\text{CH}_4^{\text{ct}}$  and  $X\text{CH}_4^{\text{ma}}$  to account for a bias between NOAA-optimized- $\text{CH}_4$  fields in TM5 and TCCON observed  $X\text{CH}_4$ , amounting to -0.76%, -0.80% and 0.59%, respectively.

We optimized monthly  $\text{CH}_4$  and  $\text{CO}_2$  fluxes for the year 2009 and 2010 by assimilating GOSAT-retrieved- $X_{\text{ratio}}$  data using the TM5-4DVAR inverse modeling system. Additional inversions, assimilating  $X\text{CH}_4^{\text{proxy}}$  and NOAA surface flask measurements were performed in a similar setup for comparison. The posterior uncertainties of the fluxes are calculated with a Monte-Carlo approach.

Overall, the ratio and proxy inversions show similar results for annual  $\text{CH}_4$  fluxes. Significant seasonal differences in  $\text{CH}_4$  are found between the two proxy inversions for TRANSCOM regions Northern Africa and Australia, which can be traced back to differences in  $X\text{CO}_2^{\text{model}}$ . The  $\text{CO}_2$  models show a systematic difference in the seasonal cycle of  $\text{CO}_2$ , resulting in a seasonally varying mismatch in the northern tropics. The ratio method has the advantage that it allows adjustment of the  $\text{CO}_2$

fluxes, whereas the proxy inversions can only account for this mismatch by adjusting  $\text{CH}_4$ . For Australia, the proxy inversions predict an anomalous  $\text{CH}_4$  increase in the second half of 2010. This difference can be explained by errors in  $\text{XCO}_2^{\text{model}}$ , which does not account for the anomalous carbon sink reported by Detmers et al. (2015) for lack of surface measurement coverage.

- 5 The ratio method has the build-in flexibility needed to attribute the anomaly to  $\text{CO}_2$  instead of  $\text{CH}_4$  and is therefore is not affected.

Inversions using satellite data show a better agreement among each other compared to the NOAA-only inversions, which use only surface data. This is true in particular for Temperate Eurasia, where the NOAA-only inversion reduces the annual  $\text{CH}_4$  flux by as much as 55 Tg/y, relative to an *a priori* flux of 121 Tg/y. This is traced back to a large overestimation of atmospheric  $\text{CH}_4$  concentration in the prior model at NOAA sites in the region, especially at Shangdianzi, where the prior model overestimates the data by 179 ppb on average. When satellite measurements are assimilated, the  $\text{CH}_4$  flux reduction for Temperate Eurasia is limited to 21 Tg/y, while accounting for the *a priori* mismatch in Shangdianzi.

- We validated the inversion-optimized atmospheric tracer fields, as well as the CarbonTracker and MACC  $\text{CO}_2$  fields used in the proxy inversions, against three independent aircraft measurement projects. For  $\text{CH}_4$ , the ratio and NOAA-only inversions showed a lower mismatch with HIPPO and AMAZONICA measurements than the two proxy inversions. Further analysis shows that this is not due to a better representation of atmospheric  $\text{CO}_2$  in the ratio inversion. However, the ratio inversion accounts for inconsistent constraints from  $X_{\text{ratio}}$  by correcting both  $\text{CH}_4$  and  $\text{CO}_2$  fluxes, whereas the proxy inversions can only attribute such constraints to  $\text{CH}_4$  fluxes. The ratio inversion predicts an enhanced  $\text{CO}_2$  natural source in this region during 2010 compared with the NOAA-only and *a priori* model. This is accordance with the findings of Gatti et al. (2014) and Vanderlaan et al. (2015), and is also supported by the AMAZONICA aircraft measurements. Overall, this study shows that the ratio method is capable of informing us about surface fluxes of  $\text{CH}_4$  and  $\text{CO}_2$  using satellite measurements, and that it provides a useful alternative for the proxy inversion method.

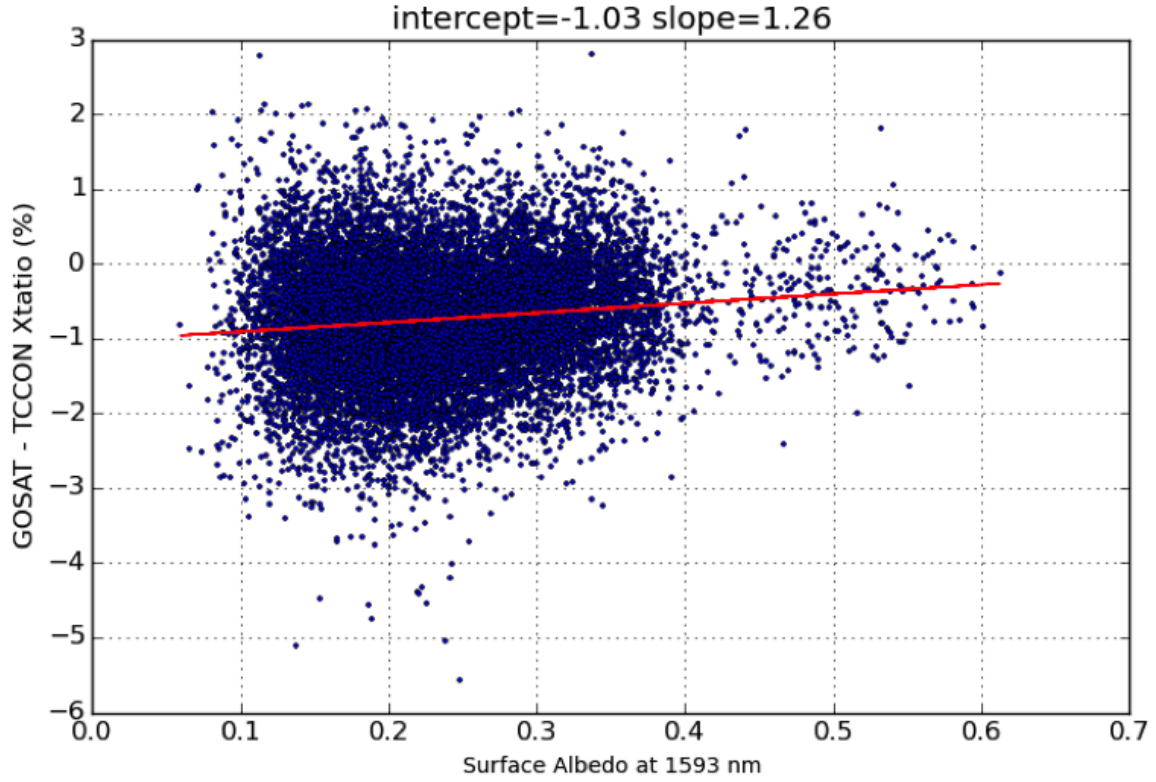


**Figure 11.** Linear regression analysis between GOSAT – TCCON  $X_{ratio}$  with Surface albedo at 1593 nm.

## Appendix A: Bias correction

We apply a two-step correction to reduce the influence of biases in our inversions:

1. **TCCON-based:** Residual biases in  $X_{ratio}$  remain that are not accounted for by taking the ratio between  $XCH_4^{ns}$  and  $XCO_2^{ns}$ . The standard bias correction procedure in the RemoTeC  $XCH_4^{proxy}$  retrieval assumes a linear dependence on surface albedo (Guerlet et al., 2013). However, this procedure would also correct biases in  $XCO_2^{model}$ , which are not expected to vary with surface albedo. Therefore, we apply the albedo-based bias correction only to the GOSAT-measured- $X_{ratio}$ . To determine the bias correction, we use GOSAT retrievals that are co-located with TCCON measurements, i.e. they are within 5 degrees latitude and longitude and within 2 hours of TCCON measurements. The relationship between surface albedo at 1593 nm and the monthly difference between GOSAT and TCCON is shown in Figure 11 . A global bias correction function is obtained by linear regression, results in a mean adjustment of  $-0.74\%$  of GOSAT  $X_{ratio}$ .

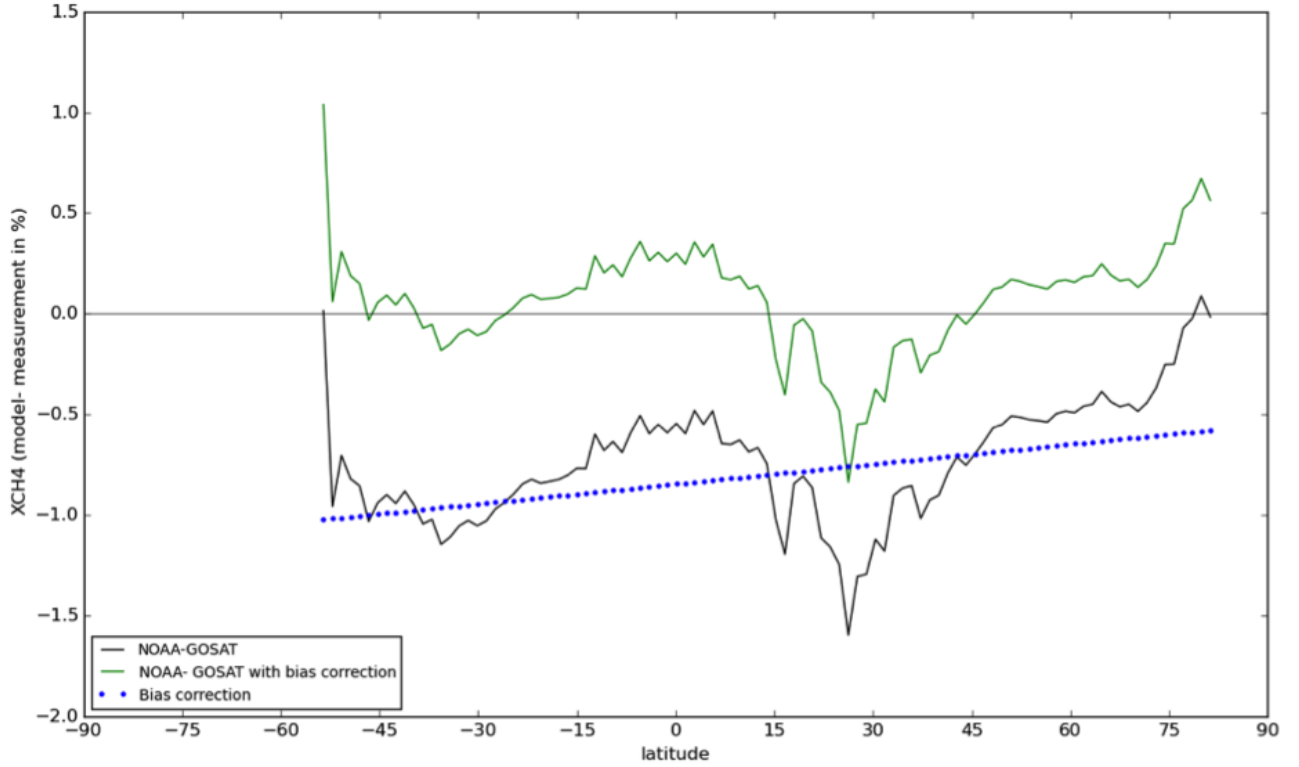


**Figure 12.** NOAA based bias correction applied to  $XCH_4$  in the PR-CT inversion

2. **NOAA-based:** A systematic mismatch between the NOAA and GOSAT-optimized TM5  $CH_4$  fields has been discussed in Monteil et al. (2013). The cause of this problem is still unresolved, but may be explained in part by transport model uncertainties in representing  $XCH_4$  in the stratosphere. Several other studies have reported similar biases and applied NOAA-based bias corrections, in addition to the TCCON derived retrieval corrections, in order to restore consistency between the observational constraints provided by surface and total column measurements (Alexe et al., 2014; Houweling et al., 2014; Basu et al., 2013). We use a similar procedure for  $X_{ratio}$  and  $XCH_4^{proxy}$  data by comparing the TCCON-corrected GOSAT retrievals to the NOAA-optimized TM5 model. The mean difference is corrected using a linear function of latitude. This results in a mean adjustment of -0.76 % in  $X_{ratio}$ , -0.59% in  $XCH_4^{ma}$  and -0.80% in  $XCH_4^{ct}$  (See Figure 12 and 13)

## Appendix B: Posterior Uncertainty

As discussed in Pandey et al. (2015), the  $X_{ratio}$  inversion problem is weakly non-linear and is solved using the quasi-Newtonian optimizer M1QN3. The standard implementation of M1QN3 does not provide an estimate of posterior uncertainty. Therefore,



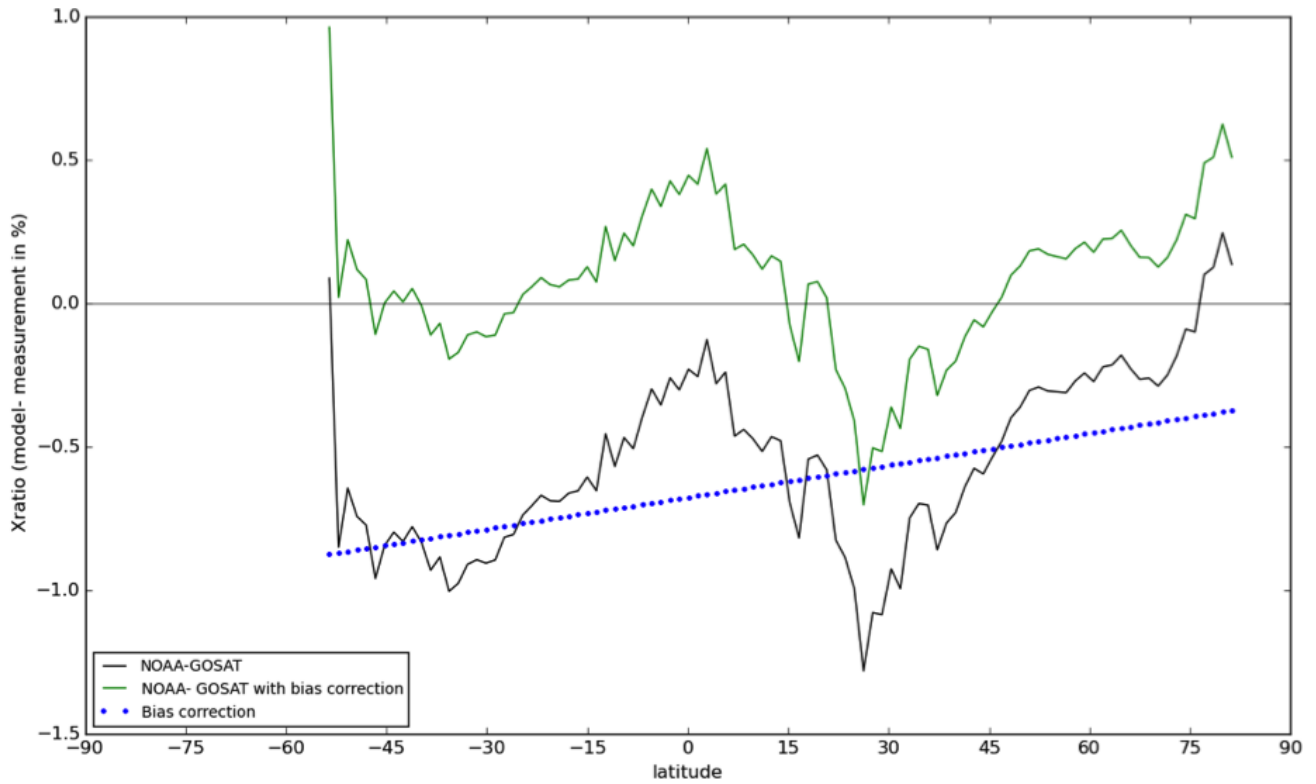


**Figure 13.** NOAA based bias correction applied to  $X_{\text{ratio}}$  in the RATIO inversion

we use the Monte-Carlo approach as described in Chevallier et al. (2007) to calculate posterior flux uncertainties. For the linear SURF and proxy inversions, which use the conjugate gradient optimization method. The posterior flux uncertainties of these inversions are derived using the same approach to keep the comparison between the uncertainties consistent. A sensitivity test has been performed to determine the size of the ensemble needed to properly capture the  $1\sigma$  of the prior fluxes. Figure 14 shows the results of this experiment. We choose an ensemble size of 24 for our experiments which gives a  $1\sigma$  estimate with 14.4 % uncertainty.

*Acknowledgements.* This work is supported by the Netherlands Organization for Scientific Research (NWO), project number ALW-GO-AO/11-24. The computations were carried out on the Dutch national supercomputer Cartesius, and we thank SURFSara ([www.surfsara.nl](http://www.surfsara.nl)) for their support. Access to the GOSAT data was granted through the third GOSAT research announcement jointly issued by JAVA, NIES, and MOE. The funding for AMAZONICA project is provided by NERC and FAPESP. We thank S. C. Wofsy for providing HIPPO data. We thank Debra Wunch and other TCCON PI's for making their measurements available.

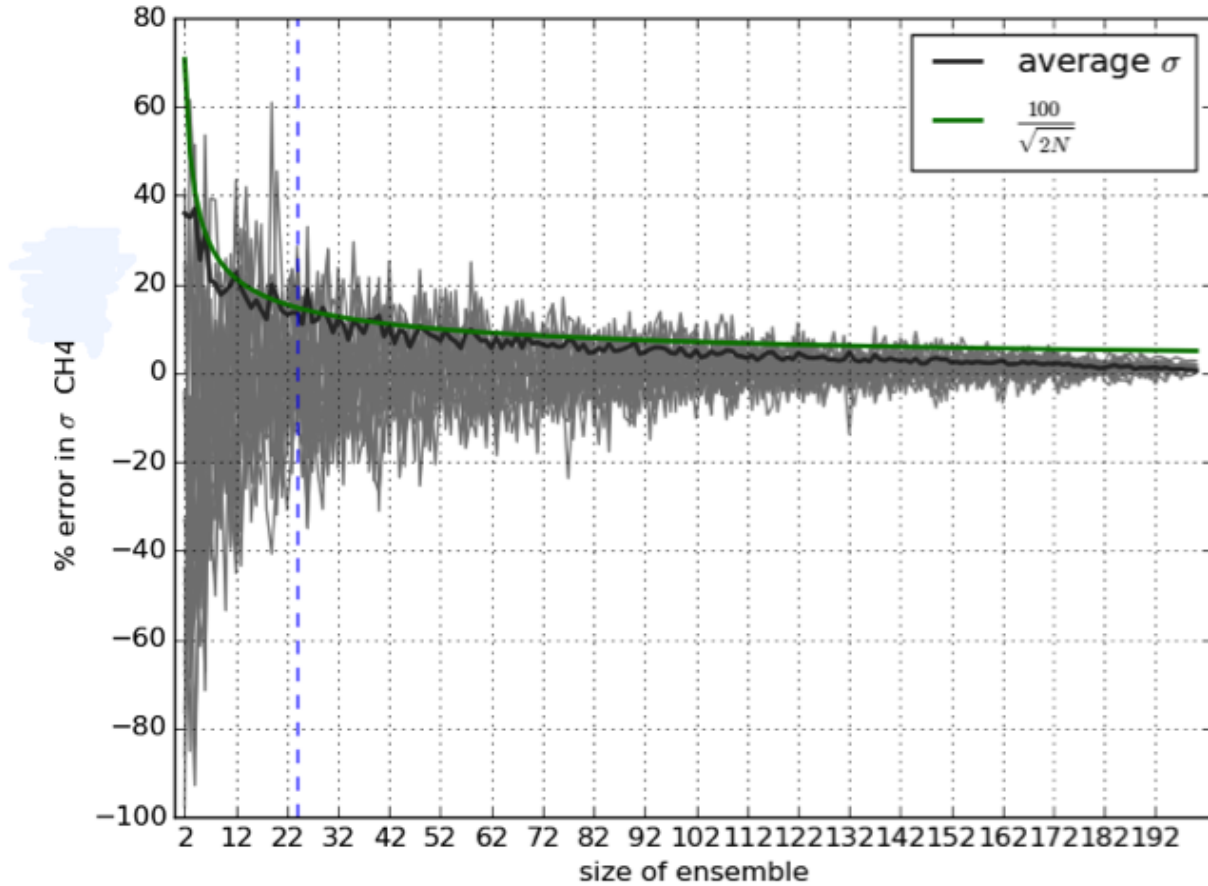


**Figure 14.** The gray lines represent the percentage error of  $\sigma$  of ensemble size  $n$  from the  $\sigma$  of ensemble size of 200 of the *a priori* CH4 flux integrated over TRANSCOM regions. The dark black line represents the average deviation in the grey lines. Green line represent the analytical variation of the uncertainty of 1  $\sigma$  (Bousserez et al., 2015). A constant difference of approx. 6% between the estimates comes from the finite size of the largest sample (200).

## References

- Alexe, M., Bergamaschi, P., Segers, A., Detmers, R., Butz, A., Hasekamp, O., Guerlet, S., Parker, R., Boesch, H., Frankenberg, C., Scheepmaker, R. A., Dlugokencky, E., Sweeney, C., Wofsy, S. C., and Kort, E. A.: Inverse modeling of CH<sub>4</sub> emissions for 2010–2011 using different satellite retrieval products from GOSAT and SCIAMACHY, *Atmospheric Chemistry and Physics Discussions*, 14, 11 493–11 539, doi:10.5194/acpd-14-11493-2014, <http://www.atmos-chem-phys-discuss.net/14/11493/2014/>, 2014.
- Basu, S., Guerlet, S., Butz, A., Houweling, S., Hasekamp, O., Aben, I., Krummel, P., Steele, P., Langenfelds, R., Torn, M., Biraud, S., Stephens, B., Andrews, A., and Worthy, D.: Global CO<sub>2</sub> fluxes estimated from GOSAT retrievals of total column CO<sub>2</sub>, *Atmospheric Chemistry and Physics*, 13, 8695–8717, doi:10.5194/acp-13-8695-2013, <http://www.atmos-chem-phys.net/13/8695/2013/>, 2013.
- Basu, S., Krol, M., Butz, A., Clerbaux, C., Sawa, Y., Machida, T., Matsueda, H., Frankenberg, C., Hasekamp, O., and Aben, I.: The seasonal variation of the CO<sub>2</sub> flux over Tropical Asia estimated from GOSAT, CONTRAIL, and IASI, *Geophysical Research Letters*, 41, 1809–1815, doi:10.1002/2013GL059105, <http://onlinelibrary.wiley.com/doi/10.1002/2013GL059105/full>, 2014.
- Bergamaschi, P., Frankenberg, C., Meirink, J. F., Krol, M., Dentener, F., Wagner, T., Platt, U., Kaplan, J. O., Körner, S., Heimann, M., Dlugokencky, E. J., and Goede, A.: Satellite cartography of atmospheric methane from SCIAMACHY on board ENVISAT: 2. Evaluation based on inverse model simulations, *Journal of Geophysical Research*, 112, D02 304, doi:10.1029/2006JD007268, <http://doi.wiley.com/10.1029/2006JD007268>, 2007.
- Bergamaschi, P., Krol, M., Meirink, J. F., Dentener, F., Segers, A., van Aardenne, J., Monni, S., Vermeulen, A. T., Schmidt, M., Ramonet, M., Yver, C., Meinhardt, F., Nisbet, E. G., Fisher, R. E., O'Doherty, S., and Dlugokencky, E. J.: Inverse modeling of European CH<sub>4</sub> emissions 2001–2006, *Journal of Geophysical Research*, 115, D22 309, doi:10.1029/2010JD014180, <http://doi.wiley.com/10.1029/2010JD014180>, 2010.
- Bergamaschi, P., Houweling, S., Segers, A., Krol, M., Frankenberg, C., Scheepmaker, R. A., Dlugokencky, E., Wofsy, S. C., Kort, E. A., Sweeney, C., Schuck, T., Brenninkmeijer, C., Chen, H., Beck, V., and Gerbig, C.: Atmospheric CH<sub>4</sub> in the first decade of the 21st century: Inverse modeling analysis using SCIAMACHY satellite retrievals and NOAA surface measurements, *Journal of Geophysical Research: Atmospheres*, 118, 7350–7369, doi:10.1002/jgrd.50480, <http://doi.wiley.com/10.1002/jgrd.50480>, 2013.
- Bousquet, P., Ciais, P., Miller, J. B., Dlugokencky, E. J., Hauglustaine, D. A., Prigent, C., Van der Werf, G. R., Peylin, P., Brunke, E.-G., Carouge, C., Langenfelds, R. L., Lathière, J., Papa, F., Ramonet, M., Schmidt, M., Steele, L. P., Tyler, S. C., and White, J.: Contribution of anthropogenic and natural sources to atmospheric methane variability., *Nature*, 443, 439–43, doi:10.1038/nature05132, <http://www.ncbi.nlm.nih.gov/pubmed/17006511>, 2006.
- Bousserez, N., Henze, D. K., Perkins, A., Bowman, K. W., Lee, M., Liu, J., Deng, F., and Jones, D. B. A.: Improved analysis-error covariance matrix for high-dimensional variational inversions: application to source estimation using a 3D atmospheric transport model, *Quarterly Journal of the Royal Meteorological Society*, 141, 1906–1921, doi:10.1002/qj.2495, <http://doi.wiley.com/10.1002/qj.2495>, 2015.
- Bruhwyler, L. M., Dlugokencky, E., Masarie, K., Ishizawa, M., Andrews, A., Miller, J., Sweeney, C., Tans, P., and Worthy, D.: CarbonTracker-CH<sub>4</sub>: an assimilation system for estimating emissions of atmospheric methane, *Atmospheric Chemistry and Physics Discussions*, 14, 2175–2233, doi:10.5194/acpd-14-2175-2014, <http://www.atmos-chem-phys-discuss.net/14/2175/2014/>, 2014.
- Butz, A., Hasekamp, O. P., Frankenberg, C., Vidot, J., and Aben, I.: CH<sub>4</sub> retrievals from space-based solar backscatter measurements: Performance evaluation against simulated aerosol and cirrus loaded scenes, *Journal of Geophysical Research*, 115, D24 302, doi:10.1029/2010JD014514, <http://doi.wiley.com/10.1029/2010JD014514>, 2010.

- Butz, A., Guerlet, S., and Hasekamp, O.: Toward accurate CO<sub>2</sub> and CH<sub>4</sub> observations from GOSAT, *Geophysical Research Letters*, 38, L14 812, doi:10.1029/2011GL047888, <http://www.agu.org/pubs/crossref/2011/2011GL047888.shtml><http://www.agu.org/journals/gl/2011/2011GL047888/2011gl047888-fs02.eps>, 2011.
- 5 Chevallier, F.: On the parallelization of atmospheric inversions of CO<sub>2</sub> surface fluxes within a variational framework, *Geoscientific Model Development Discussions*, 6, 37–57, doi:10.5194/gmdd-6-37-2013, <http://www.geosci-model-dev-discuss.net/6/37/2013/>, 2013.
- Chevallier, F., Bréon, F.-M., and Rayner, P. J.: Contribution of the Orbiting Carbon Observatory to the estimation of CO<sub>2</sub> sources and sinks: Theoretical study in a variational data assimilation framework, *Journal of Geophysical Research*, 112, D09 307, doi:10.1029/2006JD007375, <http://doi.wiley.com/10.1029/2006JD007375>, 2007.
- 10 Chevallier, F., Ciais, P., Conway, T. J., Aalto, T., Anderson, B. E., Bousquet, P., Brunke, E. G., Ciattaglia, L., Esaki, Y., Fröhlich, M., Gomez, A., Gomez-Pelaez, A. J., Haszpra, L., Krummel, P. B., Langenfelds, R. L., Leuenberger, M., Machida, T., Maignan, F., Matsueda, H., Morguí, J. A., Mukai, H., Nakazawa, T., Peylin, P., Ramonet, M., Rivier, L., Sawa, Y., Schmidt, M., Steele, L. P., Vay, S. A., Vermeulen, A. T., Wofsy, S., and Worthy, D.: CO<sub>2</sub> surface fluxes at grid point scale estimated from a global 21 year reanalysis of atmospheric measurements, *Journal of Geophysical Research*, 115, D21 307, doi:10.1029/2010JD013887, <http://doi.wiley.com/10.1029/2010JD013887>, 2010.
- 15 Chevallier, F., Palmer, P., Feng, L., Boesch, H., O'Dell, C., and Bousquet, P.: Toward robust and consistent regional CO<sub>2</sub> flux estimates from in situ and spaceborne measurements of atmospheric CO<sub>2</sub>, *Geophysical Research Letters*, 41, doi:10.1002/2013GL058772, 2014.
- Dee, D. P., Uppala, S. M., Simmons, A. J., Berrisford, P., Poli, P., Kobayashi, S., Andrae, U., Balmaseda, M. A., Balsamo, G., Bauer, P., Bechtold, P., Beljaars, A. C. M., van de Berg, L., Bidlot, J., Bormann, N., Delsol, C., Dragani, R., Fuentes, M., Geer, A. J., Haimberger, L., Healy, S. B., Hersbach, H., Hólm, E. V., Isaksen, I., Kållberg, P., Köhler, M., Matricardi, M., McNally, a. P., Monge-Sanz, B. M., Morcrette, J.-J., Park, B.-K., Peubey, C., de Rosnay, P., Tavolato, C., Thépaut, J.-N., and Vitart, F.: The ERA-Interim reanalysis: configuration and performance of the data assimilation system, *Quarterly Journal of the Royal Meteorological Society*, 137, 553–597, doi:10.1002/qj.828, <http://doi.wiley.com/10.1002/qj.828>, 2011.
- 20 Deng, F., Jones, D. B. A., Henze, D. K., Bousserez, N., Bowman, K. W., Fisher, J. B., Nassar, R., O'Dell, C., Wunch, D., Wennberg, P. O., Kort, E. A., Wofsy, S. C., Blumenstock, T., Deutscher, N. M., Griffith, D. W. T., Hase, F., Heikkinen, P., Sherlock, V., Strong, K., Sussmann, R., and Warneke, T.: Inferring regional sources and sinks of atmospheric CO<sub>2</sub> from GOSAT XCO<sub>2</sub> data, *Atmospheric Chemistry and Physics*, 14, 3703–3727, doi:10.5194/acp-14-3703-2014, 2014.
- Detmers, R. G., Hasekamp, O., Aben, I., Houweling, S., Leeuwen, T. T. V., and Butz, A.: Anomalous carbon uptake in Australia as seen by GOSAT, *Geophysical Research Letters*, 42, doi:10.1002/2015GL065161, 2015.
- 30 Deutscher, N., Notholt, J., Messerschmidt, J., Weinzierl, C., Warneke, T., Petri, C., Grupe, P., and Katrynski, K.: TCCON Data Archive, hosted by the Carbon Dioxide Information Analysis Center, Oak Ridge National Laboratory, Oak Ridge, Tennessee, USA,, <http://dx.doi.org/10.14291/tcon.ggg2014.bialystok01.R0/1149277>, 2014a.
- Deutscher, N., Notholt, J., Messerschmidt, J., Weinzierl, C., Warneke, T., Petri, C., Grupe, P., and Katrynski, K.: TCCON data from Bialystok, Poland, Release GGG2014R0. TCCON data archive, hosted by the Carbon Dioxide Information Analysis Center, Oak Ridge National Laboratory, Oak Ridge, Tennessee, U.S.A, <http://dx.doi.org/10.14291/tcon.ggg2014.bremen01.R0/1149275>, 2014b.
- 35 Frankenberg, C., Meirink, J. F., van Weele, M., Platt, U., and Wagner, T.: Assessing methane emissions from global space-borne observations., *Science (New York, N.Y.)*, 308, 1010–4, doi:10.1126/science.1106644, <http://www.ncbi.nlm.nih.gov/pubmed/15774724>, 2005.
- Frankenberg, C., Meirink, J. F., Bergamaschi, P., Goede, A. P. H., Heimann, M., Körner, S., Platt, U., van Weele, M., and Wagner, T.: Satellite chartography of atmospheric methane from SCIAMACHY on board ENVISAT: Analysis of the years 2003 and 2004, *Journal of Geo-*

- physical Research: Atmospheres, 111, n/a–n/a, doi:10.1029/2005JD006235, <http://onlinelibrary.wiley.com/doi/10.1029/2005JD006235/abstract>, 2006.
- Fraser, A., Palmer, P. I., Feng, L., Boesch, H., Cogan, A., Parker, R., Dlugokencky, E. J., Fraser, P. J., Krummel, P. B., Langenfelds, R. L., O'Doherty, S., Prinn, R. G., Steele, L. P., van der Schoot, M., and Weiss, R. F.: Estimating regional methane surface fluxes: the relative importance of surface and GOSAT mole fraction measurements, *Atmospheric Chemistry and Physics*, 13, 5697–5713, doi:10.5194/acp-13-5697-2013, <http://www.atmos-chem-phys.net/13/5697/2013/>, 2013.
- Fraser, A., Palmer, P. I., Feng, L., Bösch, H., Parker, R., Dlugokencky, E. J., Krummel, P. B., and Langenfelds, R. L.: Estimating regional fluxes of CO<sub>2</sub> and CH<sub>4</sub> using space-borne observations of XCH<sub>4</sub>: XCO<sub>2</sub>, *Atmospheric Chemistry and Physics*, 14, 12 883–12 895, doi:10.5194/acp-14-12883-2014, <http://www.atmos-chem-phys.net/14/12883/2014/>, 2014.
- Gatti, L. V., Gloor, M., Miller, J. B., Doughty, C. E., Malhi, Y., Domingues, L. G., Basso, L. S., Martinewski, A., Correia, C. S. C., Borges, V. F., Freitas, S., Braz, R., Anderson, L. O., Rocha, H., Grace, J., Phillips, O. L., and Lloyd, J.: Drought sensitivity of Amazonian carbon balance revealed by atmospheric measurements., *Nature*, 506, 76–80, doi:10.1038/nature12957, <http://www.ncbi.nlm.nih.gov/pubmed/24499918>, 2014.
- Griffith, D. W. T., Deutscher, N., Velazco, V. A., Wennberg, P. O., Yavin, Y., Aleks, G. K., Washenfelder, R., Toon, G. C., Blavier, J.-F., Murphy, C., Jones, N., Kettlewell, G., Connor, B., Macatangay, R., Roehl, C., Ryzek, M., Glowacki, J., Culgan, T., and Bryant, G.: TCCON Data from Darwin, Australia, Release GGG2014R0. TCCON Data Archive, hosted by the Carbon Dioxide Information Analysis Center, Oak Ridge National Laboratory, Oak Ridge, Tennessee, USA., <http://dx.doi.org/10.14291/tcon.ggg2014.wollongong01.R0/1149291>, 2014a.
- Griffith, D. W. T., Velazco, V. A., Deutscher, N., Murphy, C., Jones, N., Wilson, S., Macatangay, R., Kettlewell, G., Buchholz, R. R., and Riggensbach, M.: TCCON Data from Wollongong, Australia, Release GGG2014R0. TCCON Data Archive, hosted by the Carbon Dioxide Information Analysis Center, Oak Ridge National Laboratory, Oak Ridge, Tennessee, USA, <http://dx.doi.org/10.14291/tcon.ggg2014.wollongong01.R0/1149291>, 2014b.
- Guerlet, S., Butz, A., Schepers, D., Basu, S., Hasekamp, O. P., Kuze, A., Yokota, T., Blavier, J. F., Deutscher, N. M., Griffith, D. W. T., Hase, F., Kyro, E., Morino, I., Sherlock, V., Sussmann, R., Galli, A., and Aben, I.: Impact of aerosol and thin cirrus on retrieving and validating XCO<sub>2</sub> from GOSAT shortwave infrared measurements, *Journal of Geophysical Research: Atmospheres*, 118, 4887–4905, doi:10.1002/jgrd.50332, 2013.
- Gurney, K. R., Baker, D., Rayner, P., and Denning, S.: Interannual variations in continental-scale net carbon exchange and sensitivity to observing networks estimated from atmospheric CO<sub>2</sub> inversions for the period 1980 to 2005, *Global Biogeochemical Cycles*, 22, n/a–n/a, doi:10.1029/2007GB003082, <http://doi.wiley.com/10.1029/2007GB003082>, 2008.
- Hase, F., Blumenstock, T., Dohe, S., Grofl, J., and Kiel, M.: TCCON Data from Karlsruhe, Germany, Release GGG2014R0, TCCON Data Archive, hosted by the Carbon Dioxide Information Analysis Center, Oak Ridge National Laboratory, Oak Ridge, Tennessee, USA, doi:10.14291/tcon.ggg2014.karlsruhe01.R0/1149270, 2014., 2014.
- Hein, R., Crutzen, P. J., and Heimann, M.: An inverse modeling approach to investigate the global atmospheric methane cycle, *Global Biogeochemical Cycles*, 11, 43–76, doi:10.1029/96GB03043, <http://doi.wiley.com/10.1029/96GB03043>, 1997.
- Houweling, S., Kaminski, T., Dentener, F., Lelieveld, J., and Heimann, M.: Inverse modeling of methane sources and sinks using the adjoint of a global transport model, *Journal of Geophysical Research*, 104, 26 137–26 160, 1999.

- Houweling, S., Breon, F.-M., Aben, I., Rödenbeck, C., Gloor, M., Heimann, M., and Ciais, P.: Inverse modeling of CO<sub>2</sub> sources and sinks using satellite data: a synthetic inter-comparison of measurement techniques and their performance as a function of space and time, *Atmospheric Chemistry and Physics*, 4, 523–538, doi:10.5194/acp-4-523-2004, <http://www.atmos-chem-phys.net/4/523/2004/>, 2004.
- 5 Houweling, S., Krol, M., Bergamaschi, P., Frankenberg, C., Dlugokencky, E. J., Morino, I., Notholt, J., Sherlock, V., Wunch, D., Beck, V., Gerbig, C., Chen, H., Kort, E. A., Röckmann, T., and Aben, I.: A multi-year methane inversion using SCIAMACHY, accounting for systematic errors using TCCON measurements, *Atmospheric Chemistry and Physics*, 14, 3991–4012, doi:10.5194/acp-14-3991-2014, <http://www.atmos-chem-phys.net/14/3991/2014/>, 2014.
- Houweling, S., Baker, D., Basu, S., Boesch, H., Butz, A., Chevallier, F., Deng, F., Dlugokencky, E. J., Feng, L., Ganshin, A., Hasekamp, O., Jones, D., Maksyutov, S., Marshall, J., Oda, T., Dell, C. W. O., Oshchepkov, S., Palmer, P. I., Peylin, P., Poussi, Z., Reum, F., Takagi, H., Yoshida, Y., and Zhuravlev, R.: An intercomparison of inverse models for estimating sources and sinks of CO<sub>2</sub> using GOSAT measurements, *Journal of Geophysical Research*, doi:10.1002/2014JD022962, Received, 2015.
- 10 Jacobson, A. R., Mikaloff Fletcher, S. E., Gruber, N., Sarmiento, J. L., and Gloor, M.: A joint atmosphere-ocean inversion for surface fluxes of carbon dioxide: 1. Methods and global-scale fluxes, *Global Biogeochemical Cycles*, 21, n/a–n/a, doi:10.1029/2005GB002556, <http://doi.wiley.com/10.1029/2005GB002556>, 2007.
- 15 Kivi, R., Heikkinen, P., and Kyro, E.: TCCON Data from Sodankyla, Finland, Release GGG2014R0. TCCON Data Archive, hosted by the Carbon Dioxide Information Analysis Center, Oak Ridge National Laboratory, Oak Ridge, Tennessee, USA, doi:10.14291/tcon.ggg2014.sodankyla01.R0/1149280, 2014., 2014.
- Krol, M., Houweling, S., Bregman, B., van den Broek, M., Segers, A., van Velthoven, P., Peters, W., Dentener, F., and Bergamaschi, P.: The two-way nested global chemistry-transport zoom model TM5: algorithm and applications, *Atmospheric Chemistry and Physics*, 5, 417–432, doi:10.5194/acp-5-417-2005, <http://www.atmos-chem-phys.net/5/417/2005/>, 2005.
- 20 Kuze, A., Suto, H., Nakajima, M., and Hamazaki, T.: Thermal and near infrared sensor for carbon observation Fourier-transform spectrometer on the Greenhouse Gases Observing Satellite for greenhouse gases monitoring., *Applied optics*, 48, 6716–33, <http://www.ncbi.nlm.nih.gov/pubmed/20011012>, 2009.
- 25 Machida, T., Matsueda, H., Sawa, Y., Nakagawa, Y., Hirotani, K., Kondo, N., Goto, K., Nakazawa, T., Ishikawa, K., and Ogawa, T.: World-wide Measurements of Atmospheric CO<sub>2</sub> and Other Trace Gas Species Using Commercial Airlines, *Journal of Atmospheric and Oceanic Technology*, 25, 1744–1754, doi:10.1175/2008JTECHA1082.1, 2008.
- Maksyutov, S., Takagi, H., Belikov, D. A., Saeki, T., Zhuravlev, R., Ganshin, A., Lukyanov, A., Yoshida, Y., Oshchepkov, S., Bril, A., Saito, M., Oda, T., Valsala, V. K., Saito, R., Andres, R. J., Conway, T., Tans, P., and Yokota, T.: Estimation of regional surface CO<sub>2</sub> fluxes with GOSAT observations using two inverse modeling approaches , vol. 8529, pp. 85 290G–85 290G–12, <http://dx.doi.org/10.1117/12.979664>, 2012.
- 30 Meirink, J. F., Bergamaschi, P., and Krol, M. C.: Technical Note: Four-dimensional variational data assimilation for inverse modelling of atmospheric methane emissions: method and comparison with synthesis inversion, doi:10.5194/acpd-8-12023-2008, 2008.
- Monteil, G., Houweling, S., Butz, A., Guerlet, S., Schepers, D., Hasekamp, O., Frankenberg, C., Scheepmaker, R., Aben, I., and Röckmann, T.: Comparison of CH<sub>4</sub> inversions based on 15 months of GOSAT and SCIAMACHY observations, *Journal of Geophysical Research: Atmospheres*, 118, 11,807–11,823, doi:10.1002/2013JD019760, <http://doi.wiley.com/10.1002/2013JD019760>, 2013.
- 35 Morino, I., Matsuzaki, T., Ikegami, H., and Shishime, A.: TCCON data from Tsukuba, Ibaraki, Japan, 120HR, Release GGG2014R0. TCCON data archive, hosted by the Carbon Dioxide Information Analysis Center, Oak Ridge National Laboratory, Oak Ridge, Tennessee, U.S.A., doi:<http://dx.doi.org/10.14291/tcon.ggg2014.tsukuba01.R0/1149281>, 2014.

- Palmer, P. I., Suntharalingam, P., Jones, D. B. A., Jacob, D. J., Streets, D. G., Fu, Q., Vay, S. A., and Sachse, G. W.: Using CO<sub>2</sub>:CO correlations to improve inverse analyses of carbon fluxes, *Journal of Geophysical Research*, 111, D12318, doi:10.1029/2005JD006697, <http://doi.wiley.com/10.1029/2005JD006697>, 2006.
- 5 Pandey, S., Houweling, S., Krol, M., Aben, I., and Röckmann, T.: On the use of satellite-derived CH<sub>4</sub>:CO<sub>2</sub> columns in a joint inversion of CH<sub>4</sub> and CO<sub>2</sub> fluxes, *Atmospheric Chemistry and Physics*, 15, 8615–8629, doi:10.5194/acp-15-8615-2015, <http://www.atmos-chem-phys.net/15/8615/2015/>, 2015.
- Parker, R. J., Boesch, H., Byckling, K., Webb, A. J., Palmer, P. I., Feng, L., Bergamaschi, P., Chevallier, F., Notholt, J., Deutscher, N., Warneke, T., Hase, F., Sussmann, R., Kawakami, S., Kivi, R., Griffith, D. W. T., and Velazco, V.: Assessing 5 years of GOSAT Proxy XCH<sub>4</sub> data and associated uncertainties, *Atmospheric Measurement Techniques*, 8, 4785–4801, doi:10.5194/amt-8-4785-2015, <http://www.atmos-meas-tech.net/8/4785/2015/amt-8-4785-2015.html>, 2015.
- 10 Peters, W., Jacobson, A. R., Sweeney, C., Andrews, A. E., Conway, T. J., Masarie, K., Miller, J. B., Bruhwiler, L. M. P., Pétron, G., Hirsch, A. I., Worthy, D. E. J., van der Werf, G. R., Randerson, J. T., Wennberg, P. O., Krol, M. C., and Tans, P. P.: An atmospheric perspective on North American carbon dioxide exchange: CarbonTracker., *Proceedings of the National Academy of Sciences of the United States of America*, 104, 18925–18930, doi:10.1073/pnas.0708986104, 2007.
- 15 Reuter, M., Buchwitz, M., Hilker, M., Heymann, J., Schneising, O., Pillai, D., Bovensmann, H., Burrows, J. P., Bösch, H., Parker, R., Butz, A., Hasekamp, O., O'Dell, C. W., Yoshida, Y., Gerbig, C., Nehrkorn, T., Deutscher, N. M., Warneke, T., Notholt, J., Hase, F., Kivi, R., Sussmann, R., Machida, T., Matsueda, H., and Sawa, Y.: Satellite-inferred European carbon sink larger than expected, *Atmospheric Chemistry and Physics*, 14, 13739–13753, doi:10.5194/acp-14-13739-2014, <http://www.atmos-chem-phys.net/14/13739/2014/>, 2014.
- 20 Schepers, D., Guerlet, S., Butz, A., Landgraf, J., Frankenberg, C., Hasekamp, O., Blavier, J.-F., Deutscher, N. M., Griffith, D. W. T., Hase, F., Kyro, E., Morino, I., Sherlock, V., Sussmann, R., and Aben, I.: Methane retrievals from Greenhouse Gases Observing Satellite (GOSAT) shortwave infrared measurements: Performance comparison of proxy and physics retrieval algorithms, *Journal of Geophysical Research*, 117, D10307, doi:10.1029/2012JD017549, <http://doi.wiley.com/10.1029/2012JD017549>, 2012.
- Sherlock, V., Connor, B., Robinson, J., Shiona, H., Smale, D., and Pollard, D.: TCCON Data from Lauder, New Zealand, 120HR, Release GGG2014R0. TCCON Data Archive, hosted by the Carbon Dioxide Information Analysis Center, Oak Ridge National Laboratory, Oak Ridge, Tennessee, USA, doi:<http://dx.doi.org/10.14291/tcon.ggg2014.lauder01.R0/1149293>, Lauder, 2014.
- 25 Spahni, R., Wania, R., Neef, L., van Weele, M., Pison, I., Bousquet, P., Frankenberg, C., Foster, P. N., Joos, F., Prentice, I. C., and van Velthoven, P.: Constraining global methane emissions and uptake by ecosystems, *Biogeosciences*, 8, 1643–1665, doi:10.5194/bg-8-1643-2011, <http://www.biogeosciences.net/8/1643/2011/>, 2011.
- 30 Sussmann, R. and Rettinger, M.: TCCON Data from Garmisch, Germany, Release GGG2014R0. TCCON Data Archive, hosted by the Carbon Dioxide Information Analysis Center, Oak Ridge National Laboratory, Oak Ridge, Tennessee, USA, doi:<http://dx.doi.org/10.14291/tcon.ggg2014.garmisch01.R0/1149299>, 2014.
- Thompson, R. L., Stohl, A., Zhou, L. X., Dlugokencky, E., Fukuyama, Y., Tohjima, Y., Kim, S., Lee, H., Nisbet, E. G., Fisher, R. E., Lowry, D., Weiss, R. F., Prinn, R. G., Doherty, S. O., Young, D., and White, J. W. C.: Methane emissions in East Asia for 2000–2011 estimated using an atmospheric Bayesian inversion, *Journal of Geophysical Research*, 120, 4352–4369, doi:10.1002/2014JD022394, Received, 2015.
- 35 Turner, A. J., Jacob, D. J., Wecht, K. J., Maasakkers, J. D., Lundgren, E., Andrews, A. E., Biraud, S. C., Boesch, H., Bowman, K. W., Deutscher, N. M., Dubey, M. K., Griffith, D. W. T., Hase, F., Kuze, A., Notholt, J., Ohyama, H., Parker, R., Payne, V. H., Sussmann, R., Sweeney, C., Velazco, V. A., Warneke, T., Wennberg, P. O., and Wunch, D.: Estimating global and North American methane emissions with

- high spatial resolution using GOSAT satellite data, *Atmospheric Chemistry and Physics*, 15, 7049–7069, doi:10.5194/acp-15-7049-2015, <http://www.atmos-chem-phys.net/15/7049/2015/>, 2015.
- Vanderlaan, I. T., VanderVelde, I. R., Krol, M. C., Gatti, L. V., Domingues, L. G., Correia, C. S. C., Miller, J. B., Gloor, M., Leeuwen, T. T., Kaiser, J. W., Wiedinmyer, C., Basu, S., Clerbaux, C., and Peters, W.: Response of the Amazon carbon balance to the 2010 drought derived with CarbonTracker South America, *Global Biogeochemical Cycles*, 29, 1–17, doi:10.1002/2014GB005082. Received, 2015.
- Warneke, T., Messerschmidt, J., Notholt, J., Weinzierl, C., Deutscher, N., Petri, C., Grupe, P., Vuillemin, C., Truong, F., Schmidt, M., Ramonet, M., and E., P.: TCCON Data from Orleans, France, Release GGG2014R0. TCCON Data Archive, hosted by the Carbon Dioxide Information Analysis Center, Oak Ridge National Laboratory, Oak Ridge, Tennessee, USA, doi:10.14291/tcon.ggg2014.orleans01.R0/1149276, 2014., 2014.
- Wennberg, P. O., Roehl, C., Wunch, D., Toon, G. C., Blavier, J.-F., Washenfelder, R., Keppel-Aleks, G., Allen, N., and Ayers, J.: TCCON data from Park Falls, Wisconsin, USA, Release GGG2014R0. TCCON data archive, hosted by the Carbon Dioxide Information Analysis Center, Oak Ridge National Laboratory, Oak Ridge, Tennessee, U.S.A, doi:10.14291/tcon.ggg2014.parkfalls01.R0/1149161, 2014a.
- Wennberg, P. O., Wunch, D., Roehl, C., Blavier, J.-F., Toon, G. C., Allen, N., Dowell, P., Teske, K., Martin, C., and Martin, J.: TCCON Data from Lamont, Oklahoma, USA, Release GGG2014R0. TCCON Data Archive, hosted by the Carbon Dioxide Information Analysis Center, Oak Ridge National Laboratory, Oak Ridge, Tennessee, USA, doi:<http://dx.doi.org/10.14291/tcon.ggg2014.lamont01.R0/1149159>, 2014b.
- Wofsy, S. C., Daube, B. C., Jimenez, R., Kort, E., Pittman, J. V., Park, S., Commane, R., Xiang, B., Santoni, G., Jacob, D., Fisher, J., Pickett-Heaps, C., Wang, H., Wecht, K., Wang, Q.-Q., Stephens, B. B., Shertz, S., Watt, A., Romashkin, P., Campos, T., Haggerty, J., Cooper, W. A., Rogers, D., Beaton, S., Hendershot, R., Elkins, J. W., Fahey, D. W., Gao, R. S., Moore, F., Montzka, S. A., Schwarz, J. P., Perring, A. E., Hurst, D., Miller, B. R., Sweeney, C., Oltmans, S., Nance, D., Hints, E., Dutton, G., Watts, L. A., Spackman, J. R., Rosenlof, K. H., Ray, E. A., Hall, B., Zondlo, M. A., Diao, M., Keeling, R., Bent, J., Atlas, E. L., Lueb, R., and Mahoney, M. J.: HIPPO Merged 10-second Meteorology, Atmospheric Chemistry, Aerosol Data (R\_20121129). Carbon Dioxide Information Analysis Center, Oak Ridge National Laboratory, Oak Ridge, Tennessee, U.S.A., doi:[http://dx.doi.org/10.3334/CDIAC/hippo\\_010](http://dx.doi.org/10.3334/CDIAC/hippo_010), 2012a.
- Wofsy, S. C., Daube, B. C., Jimenez, R., Kort, E., Pittman, J. V., Park, S., Commane, R., Xiang, B., Santoni, G., Jacob, D., Fisher, J., Pickett-Heaps, C., Wang, H., Wecht, K., Wang, Q.-Q., Stephens, B. B., Shertz, S., Watt, A., Romashkin, P., Campos, T., Haggerty, J., Cooper, W. A., Rogers, D., Beaton, S., Hendershot, R., Elkins, J. W., Fahey, D. W., Gao, R. S., Moore, F., Montzka, S. A., Schwarz, J. P., Perring, A. E., Hurst, D., Miller, B. R., Sweeney, C., Oltmans, S., Nance, D., Hints, E., Dutton, G., Watts, L. A., Spackman, J. R., Rosenlof, K. H., Ray, E. A., Hall, B., Zondlo, M. A., Diao, M., Keeling, R., Bent, J., Atlas, E. L., Lueb, R., and Mahoney, M. J.: HIPPO NOAA Flask Sample GHG, Halocarbon, and Hydrocarbon Data (R\_20121129). Carbon Dioxide Information Analysis Center, Oak Ridge National Laboratory, Oak Ridge, Tennessee, U.S.A., doi:[http://dx.doi.org/10.3334/CDIAC/hippo\\_013](http://dx.doi.org/10.3334/CDIAC/hippo_013), 2012b.
- Wunch, D., Toon, G. C., Blavier, J.-F. L., Washenfelder, R. A., Notholt, J., Connor, B. J., Griffith, D. W. T., Sherlock, V., and Wennberg, P. O.: The total carbon column observing network., *Philosophical transactions. Series A, Mathematical, physical, and engineering sciences*, 369, 2087–112, doi:10.1098/rsta.2010.0240, <http://www.ncbi.nlm.nih.gov/pubmed/21502178>, 2011.
- Yokota, T., Yoshida, Y., Eguchi, N., Ota, Y., Tanaka, T., Watanabe, H., and Maksyutov, S.: Global Concentrations of CO<sub>2</sub> and CH<sub>4</sub> Retrieved from GOSAT: First Preliminary Results, *SOLA*, 5, 160–163, doi:10.2151/sola.2009-041, [https://www.jstage.jst.go.jp/article/sola/5/0/5\\_0\\_160/\\_article](https://www.jstage.jst.go.jp/article/sola/5/0/5_0_160/_article), 2009.



Yoshida, Y., Ota, Y., Eguchi, N., Kikuchi, N., Nobuta, K., Tran, H., Morino, I., and Yokota, T.: Retrieval algorithm for CO<sub>2</sub> and CH<sub>4</sub> column abundances from short-wavelength infrared spectral observations by the Greenhouse gases observing satellite, *Atmospheric Measurement Techniques*, 4, 717–734, doi:10.5194/amt-4-717-2011, <http://www.atmos-meas-tech.net/4/717/2011/>, 2011.